Catalysis Today 330 (2019) 2–15

Contents lists available at ScienceDirect

Catalysis Today

journal homepage: www.elsevier.com/locate/cattod

Intermetallics in catalysis: An exciting subset of multimetallic catalysts

Anish Dasgupta[a], Robert M. Rioux[a,b,*]

[a] Department of Chemical Engineering, The Pennsylvania State University, PA, 16801, USA
[b] Department of Chemistry, The Pennsylvania State University, PA, 16801, USA

ARTICLE INFO

Keywords:
Intermetallics
Alloy
Catalysis
Active site
Site isolation
Pd-Zn
Selective hydrogenation

ABSTRACT

In this article, we highlight the growing application of intermetallic compounds in heterogeneous catalysis. We clearly discuss intermetallics as distinct from other multi-metallic systems (such as alloys, surface modifiers and dopants). Intermetallics possess a number of attributes over random alloys (i.e., solid solutions) and serve as model catalysts for a number of industrially relevant reactions. We review a variety of methods used for the synthesis of a large number of intermetallic compounds and discuss how standard material characterization techniques can be extended to intermetallics to gain important insight regarding active site morphology, a critical metric in heterogeneous catalyst design. We further summarize the use of intermetallics in understanding changes in reactivity and selectivity due to geometric and electronic effects, with emphasis on determining compositional and structural factors of the active site. We conclude with a brief summary of avenues for future advances in the field and its potential to contribute to environment and economy.

1. Introduction

It has been known to humankind for the past 5000 years that melting two metals together followed by cooling to re-solidify leads to the formation of new materials with properties distinct from either of the constituent metals. The first example of such a material is bronze (88% Cu + 12% Sn) which was found to be much harder and more suited for making tools and weaponry than pure Cu [1]. Since then countless alloys have been utilized in important applications (with steel being arguably the most important) throughout human history because of their unique, emergent properties.

1.1. A brief introduction to phase diagram, alloys and intermetallic compounds

It is only rather recent the term “intermetallic” has started being used in its technically correct sense rather than as synonym for “alloy” [2]. An intermetallic is a solid phase containing at least two metals having a well-defined crystal structure with fixed atom positions and site occupancies[1] leading to long range ordering. An alloy is a random substituted solid solution of at least two metals where the atomic site distribution of the constituent elements is not fixed. In this case, the site occupancy is likely to be a statistical distribution dependent upon stoichiometry. Fig. 1 illustrates the difference between an intermetallic and random alloy. Fig. 1a is the PdZn intermetallic structure (P4/mmm) with Pd at (0, 0, 0) and Zn at (0.5, 0.5, 0.5) while Fig. 1b represents a random alloy without any long range symmetry.

A primary reason for the well-defined periodicity of intermetallics is the strong ionic/electronic interaction between its constituents. These interactions promote formation of unique and complex crystal structures distinct from either of the parent metals, whereas in an alloy the crystal structure of the more abundant parent material (solvent) is expected to be retained. For example, in the Ni-Ru phase diagram, alloys up to 31 at % Ru retain the FCC Ni structure (Fm-3 m) while alloys containing > 51 at% Ru crystallize in the HCP Ru structure ($P6_3$/mmc). This binary system has no intermetallic phases [3]. On the other hand, intermetallic NiZn has space group P4/mmm and Ni_4Zn_{22} has space group I-43 m, which are distinctly different from Ni (Fm-3 m) and Zn ($P6_3$/mmc).

Hume-Rothery has suggested that the crystal structure of many intermetallics are primarily determined by the valence electron concentration (*vec*), which is defined as the number of valence electrons/atom in a unit cell. Valence electron charge is based only on the number of valence *s* and *p* electrons. For example, Al ($[Ne]3s^23p^1$) contributes 3 electrons, Zn ($[Ar]3d^{10}4s^2$) contributes 2, Au ($[Xe]4f^{14}5d^{10}6s^1$) contributes 1 and Pd contributes 0 ($[Kr]4d^{10}5s^\circ$) [4]. For *vec* = 1.5, the

* Corresponding author at: Department of Chemical Engineering, The Pennsylvania State University, PA 16801, USA.
E-mail address: rioux@engr.psu.edu (R.M. Rioux).

[1] In this review the word “site” is used both from the perspective of catalysis and crystallography but there is a subtle difference in the usage of this word in these two fields. In crystallography “site” means all lattice positions related by the specific crystallographic (space group) symmetry. In catalysis “site” refers to a cluster of atoms on the surface where a chemical reaction is being catalyzed. For clarity we have used the word active site when referring to the latter case.

https://doi.org/10.1016/j.cattod.2018.05.048
Received 12 March 2018; Received in revised form 30 April 2018; Accepted 23 May 2018
Available online 24 May 2018
0920-5861/

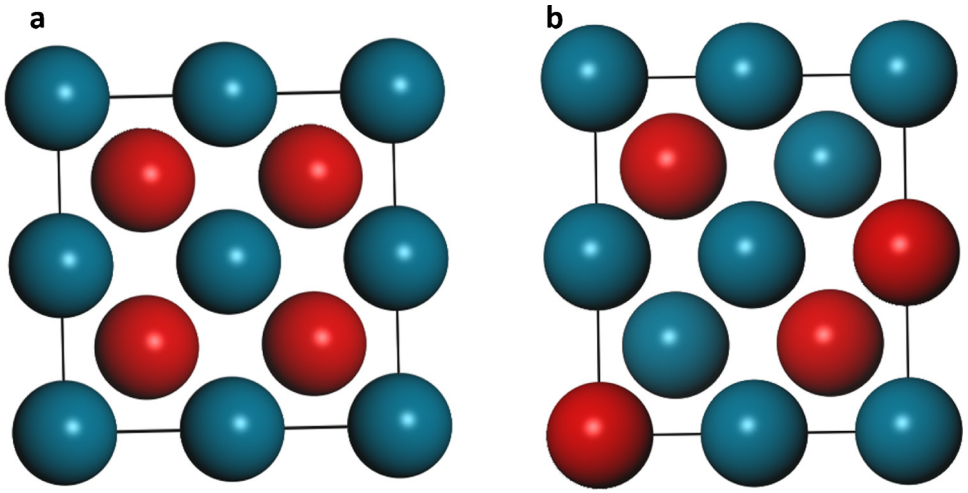

Fig. 1. Schematic diagram of (a) an ordered intermetallic (in particular PdZn structure) and (b) an alloy without any periodic order or well-defined site occupation. Blue and red balls are Pd and Zn, respectively (For interpretation of the references to colour in this figure legend, the reader is referred to the web version of this article).

structure is bcc, for *vec* = 1.61 it is γ-brass and for *vec* = 1.75 the structure is hcp. Many intermetallics follow these guidelines and are called Hume-Rothery phases [5]. The stability of Hume-Rothery phases arise from the electronic density of state (DOS) of the specific compounds. It is believed Hume-Rothery conditions leads to the formation of pseudo-gaps near the fermi-level due to the FsBz (Fermi surface-Brillouin zone) interaction, which in turn leads to the stabilization of the particular structure predicted by the Hume-Rothery rule. However, the origin of the exceptional stability of such Hume-Rothery phases is not fully understood and it can't be satisfactorily explained why even minor deviations from these *vec* values lead to increased structural disorder and the formation of unusually large unit cells which are effectively superstructures [4]. A detailed discussion on the origin of the stability of Hume-Rothery phases is presented elsewhere [6,7]. Though intermetallics are not required to follow the Hume-Rothery rules (and all compounds that follow the Hume-Rothery rules are not necessarily intermetallics), the concept of electronic structure guided phase formation is particularly relevant in catalysis (see below and Section 4) and most intermetallic catalysts used to date are Hume-Rothery phases.

The same bi (multi)-metallic system can contain both intermetallic and alloy phases as shown in Fig. 2a for the Ni-Zn system [8]. Further, in the Ni-Zn phase diagram, both the intermetallic and alloy phases exist over a range of compositions rather than only particular ratios of Ni to Zn. Alternately some metal systems may have no tendency to form any intermetallic phase as shown in Fig. 2b for Pd-Ag [9]. Often only intermetallic line compounds (single specific composition) are present but no phase-pure alloy is formed for certain metal combinations. For example the only homogenous bimetallic phase[2] in the Al-As system is the line compound, AlAs [10]. Any other finite ratio of Al:As leads to mixed phases as shown in Fig. 2c. This case is distinct from an alloy. For example, the alloy having a nominal composition Ni_4Zn is phase pure (although disordered with respect to atomic site occupation of Ni and Zn in the lattice) and only shows XRD peaks characteristic of space group Fm-3 m (same as Ni except for a possible slight 2θ shift associated with a small change in lattice constant due to alloying). However, a material with a nominal composition of Al_3As_7 will show peaks for both AlAs and pure As.

For the same composition a phase may switch between intermetallic and alloy as a function of temperature. For example a nominal composition of Au_3Cu is intermetallic below 200 °C but becomes a random alloy at higher temperature [3].

1.2. Role of intermetallics and alloys in catalysis

The application of alloys in catalysis is a rather recent development (compared to thermal and mechanical applications). Alloying can affect the catalytic properties of a material by modifying both the active site morphology (geometric effect) and electronic structure as discussed below. The geometric effect of alloying essentially stems from the fact that many commercially important reactions are either structure sensitive at an atomistic level (for example Yardimci et al. [11] found that the nuclearity of Ru clusters have a large effect on butadiene semi-hydrogenation selectivity) or requires a certain chemical environment (i.e. composition) at the gas-solid interface for optimal performance (for example, McCue et al. [12] found that exposing both Cu and Pd on the catalyst surface in the right proportion balances the over-hydrogenation propensity of Pd with the oligomerization tendency of Cu to yield a highly selective acetylene semi-hydrogenation catalyst). It is therefore intuitive that a suitable bi-metallic (or multi-metallic) alloy may have significant catalytic applications. For example, Pd-Ag alloys are the standard industrial catalyst for acetylene semi-hydrogenation because the presence of silver (typically ~ 67%) reduces the interaction between the hydrocarbon feed and the catalyst surface by breaking up large Pd clusters, thereby limiting over-hydrogenation [13].

Apart from geometric effects (i.e., crystallographic site isolation), change in electronic structure (due to charge transfer and hybridization effect as a result of varying coordination environment) during alloying can also affect the interaction of the surface with the reactants which may in turn influence catalytic properties. For example, Neurock and co-workers [14] calculated the charge transfer from Ag to the *d*-orbital of Pd in a Pd-Ag alloy reduces the binding energy of alkynes by 10–20 kJ/mole in addition to the ~35 kJ/mole reduction attributed to geometric ensemble (site isolation) effects mentioned previously.

Typically, both geometric and electronic effects occur simultaneously as a result of alloying. In a recent perspective Meyer et al. [15] has deconvoluted these two effects and highlighted their individual impact towards driving selectivity of catalytic reactions. The primary conclusion was electronic effects can alter interaction of the surface with the reactants, but they cannot break positive correlations between adsorption energy of desired and undesired intermediates (which is the main cause of non-selectivity in pure metals) and can thus only provide incremental benefits [16]. However, geometric effects can break such correlations and have a much stronger impact on selectivity. Further details of these effects are presented in reviews by Sinfelt [17] and Norskov and co-workers [18,19].

[2] In this review (and consistent with traditional crystallography literature) a "homogenous phase" means either an alloy or an intermetallic. It simply refers to homogeneity in terms of space group symmetry in a particular region of the phase diagram. Unless otherwise mentioned, it does not refer to atomic level homogeneity associated with atomic site distribution.

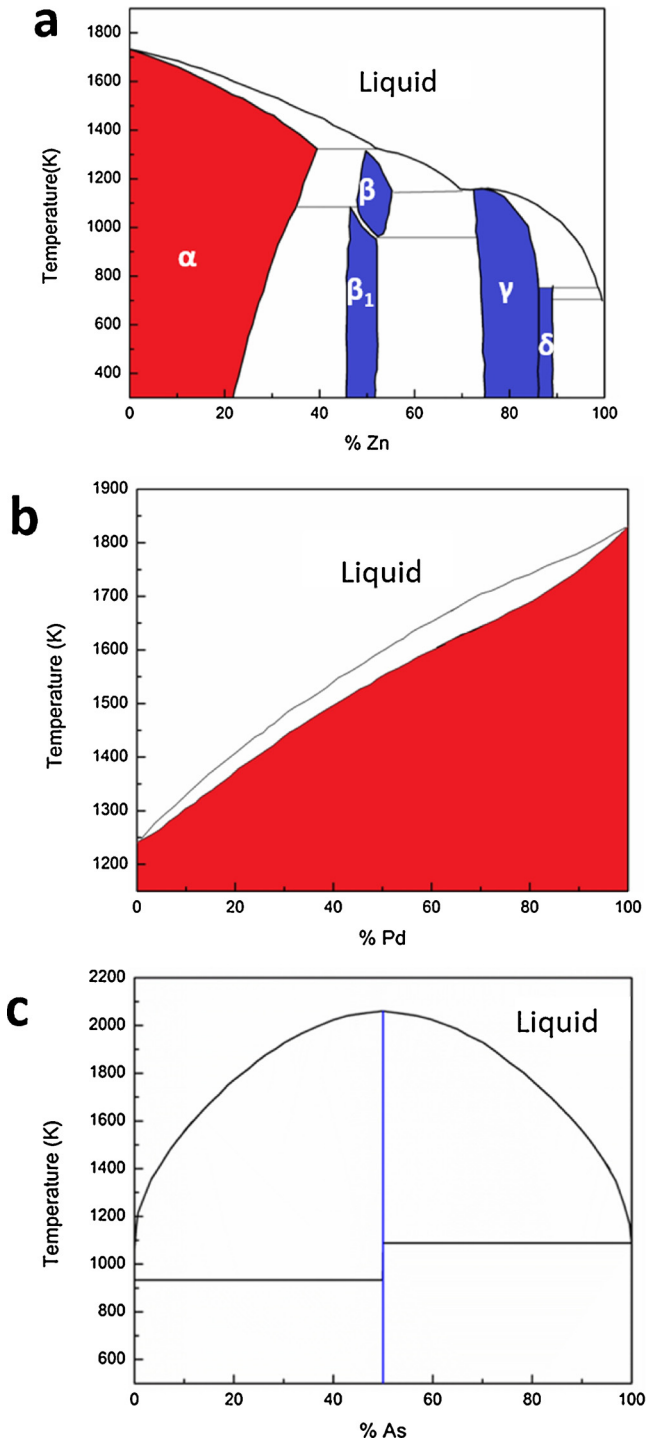

Fig. 2. Phase diagrams of (a) Ni-Zn (reprinted with permission from reference [8], copyright 2000, ASM International.), (b) Pd-Ag (reprinted with permission from reference [9], copyright 1988, Springer) and (c) Al-As (reprinted with permission from reference [10], copyright 1984, ASM International). Blue regions (in (a)) or line (in (c)) indicates intermetallic phases while red regions (in (a) and (b)) indicate alloys. Uncolored regions indicate non-homogenous compositions. Compositions are in atom% (For interpretation of the references to colour in this figure legend, the reader is referred to the web version of this article).

1.3. Advantages of intermetallics over alloys in catalysis

It is even more advantageous to use an intermetallic than an alloy because the unique crystal structure and long range atomic ordering in an intermetallic ensures (in theory) homogenous and reproducible active site morphology and allows greater control on catalyst design. This essential difference between the two types of phase pure bi (multi)-metallics is the motivation for specifically calling intermetallics as model catalysts. At this point it is worth highlighting that the surface composition may vary with respect to the bulk (discussed in Section 3) and the long range periodic order in the crystal lattice may be perturbed at the surface depending on reaction temperature and chemical atmosphere. The exact relationship between bulk and surface (active site) configurations in intermetallics has not been studied in detail and is likely difficult to achieve as the surface morphology can be altered even in the presence of a few ppm of an impurity such as oxygen. [20] However, Meyer et al. [15] has argued (consistent with the suggestion by Kovnir et al. [2]) the "enthalpic driving force" of intermetallics to maintain their structure inhibits surface segregation effects compared to alloys and they are thus expected to serve as better model systems.

In addition to greater atomic ordering, intermetallics can also form unique crystal structures (Fig. 3) which are not commonly demonstrated by alloys (or pure metals) and may be advantageous to catalysis due to favorable geometric or electronic effects. For example the γ-brass phase (Fig. 3c) seen in many transition metal phase diagrams has a distinct crystal structure [21] leading to unique coordination geometries and hence active site morphology as discussed in Sections 3 and 4 for γ-brass Ni-Zn.

The advantage of intermetallic over an alloy for catalysis was succinctly demonstrated by Armbruster et al. [22] It is well-documented the nuclearity of the active site has a strong influence on acetylene semi-hydrogenation selectivity. In their paper, two $Cu_{60}Pd_{40}$ catalysts were tested with Pd being considered the "active element" (since it is a significantly more active hydrogenation catalyst than Cu due to the activated nature of H_2 dissociation on Cu [23]). Despite having identical compositions, one bimetallic was a disordered alloy with an FCC structure (similar to the solvent, Cu) while the other crystallized into an ordered CsCl structure (intermetallic). This was achieved by annealing the same bimetallic powder at different temperatures (800 °C for alloy and 200 °C for intermetallic) for 2–3 weeks. The intermetallic had a higher Pd-Pd separation (0.29624 nm compared to 0.26436 nm) resulting in greater extent of site isolation and higher ethylene selectivity (90% versus 75% at ~90% acetylene conversion).

Such direct comparison between alloy and intermetallic of same composition is rare in the literature and it is much more common to compare alloy/intermetallic with their pure constituent elements as discussed in subsequent sections. Interestingly, Tsai et al. [24–26] has identified that certain intermetallics have identical DOS as a third catalytic metal and may be used as a direct replacement for catalyzing relevant chemistries. For example, the performance of PdZn and PdCd for methanol steam reforming is exactly similar to pure Cu (due to similarity in the DOS of the three materials) and distinctly different from Pd.

An additional advantage of intermetallics is their well-defined periodic structure makes them much more tenable towards density functional theory (DFT) calculations [27,28] (which utilizes infinitely repeated periodic structure in 3-D) compared to alloys. In fact intermetallics have also been used as quasi-crystal approximants because of the ease of computing associated with their long range order [29].

Intermetallics are typically mechanically hard and brittle, have high melting points and desirable electronic, magnetic and chemical properties distinct from the parent metals [30–34]. Over the past four decades (and from around the same time as the conception of the term "intermetallic"), intermetallics have been used in a wide variety of mechanical, electrical and thermal applications with its most common chemical application being hydrogen storage and corrosion resistance. These applications are detailed elsewhere [30,34–36] and beyond the scope of this review. In recent times, intermetallics have enjoyed exponentially increasing popularity as catalysts in academia (as

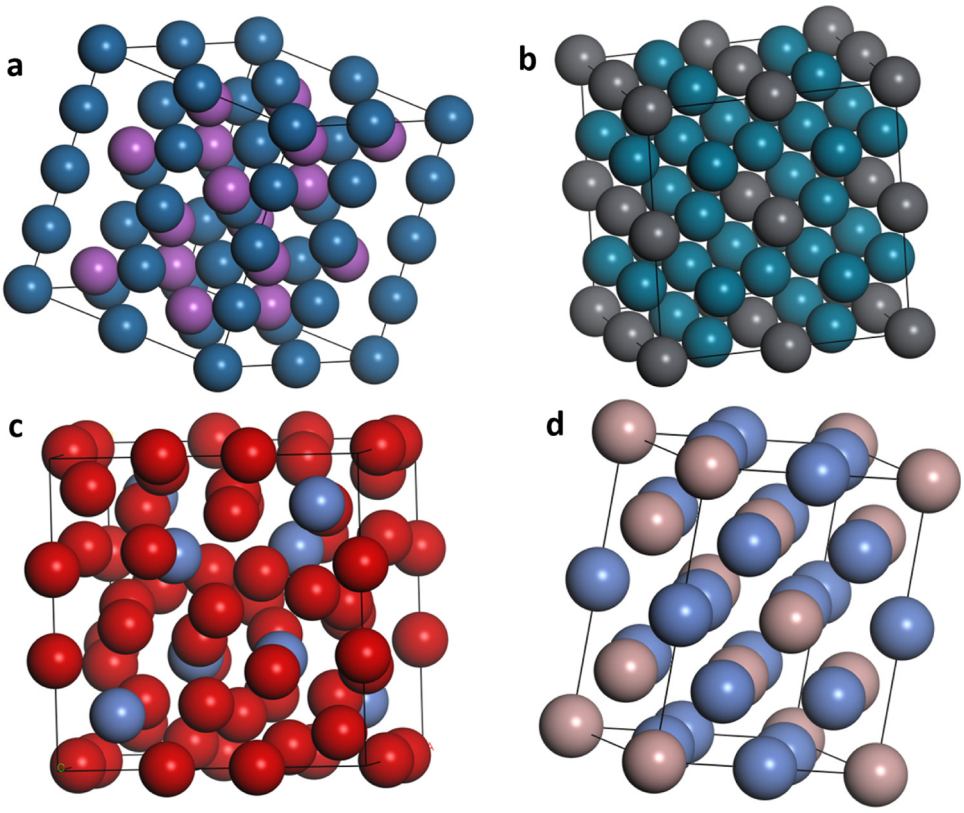

Fig. 3. Crystal structures of some catalytically relevant intermetallic phases. (a) PtBi (2 × 2 × 2 cell), (b) Pd_3Pb (2 × 2 × 2 cell), (c) Ni_2Zn_{11} (unit cell) and (d) Ni_5Ga_3 (unit cell). Dark blue atoms are Pt, dark pink atoms are Bi, grey atoms are Ni, red atoms are Zn, light pink atoms are Ga, black atoms are Pb and green atoms are Pd (For interpretation of the references to colour in this figure legend, the reader is referred to the web version of this article).

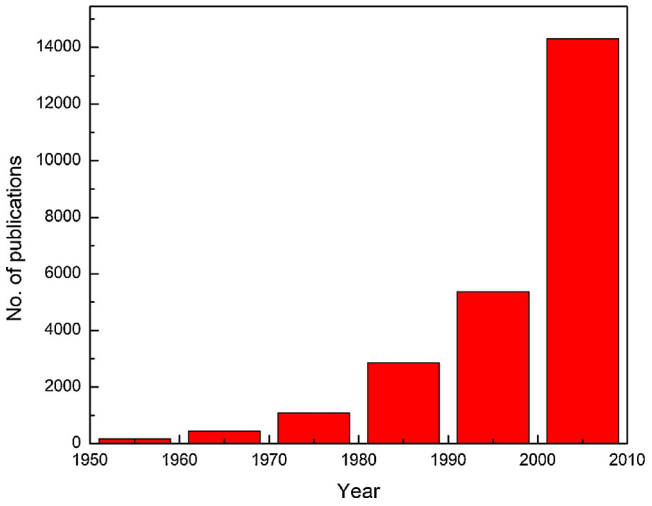

Fig. 4. Approximate number of publication for search words "intermetallic catalyst" on Google Scholar by decade.

illustrated in Fig. 4) and industry. Table 1 summarizes a number of intermetallic compounds and the relevant chemistries they catalyze better than the respective traditional catalysts (see Section 4 for detailed discussions). The remainder of this paper is dedicated to the review of these intermetallics in catalysis including various synthesis strategies, proper characterization techniques and representative examples.

2. Synthesis of intermetallic compounds

The synthesis of monometallic catalysts (typically supported nanoparticles, NP) through wet or dry impregnation techniques is well-known [54–57] and reviewed in detail in the literature [58,59]. Conversely, methods for synthesizing intermetallic catalysts are not well established. Researchers have discovered a number of approaches to synthesize intermetallic compounds of desired stoichiometry with high phase purity but these techniques are not often transferable between metal pairs or composition ranges. A particular method is effective for a limited number of bimetallic systems.

The most traditional technique for the synthesis of intermetallic compounds is through bulk thermal diffusion [2,4,60–62]. By this technique the two constituent elements (preferably of high purity) are physically mixed in a crucible and heated under vacuum for a prolonged period of time (up to a week) at a temperature of above 700 °C. The high temperature facilitates thermal diffusion of one metal into another leading to the formation of an alloy/intermetallic. The approach is easily extended to multi-metallic systems by simple modification of the composition of the starting mixture [4,61]. This technique results in thermodynamic equilibrium phases (because of the intrinsically slow solid diffusion step and high synthesis temperature) and phase-pure materials can only be obtained if the starting ratios fall within the range of a single phase. As demonstrated in Fig. 2a, a starting composition of 40 at % Ni will result in a mixture of γ and β phases while a starting composition of 17 at% Ni will result in phase pure γ material provided of course synthesis time and temperature are adequate for bulk thermal diffusion. Further, the cooling rate may also become important in certain cases. A fast cooling step would result in a kinetic (rather than thermodynamic) control and phase impure materials will begin to form based on the tie-line rule as the mixture passes through different phase regimes while cooling down. For example, we found the synthesis of Ni_5Ga_3 phase requires a temperature of 1000 °C for effective thermal diffusion. However, the phase is only stable until about 700 °C. A fast cooling (typically achieved by simply shutting off the furnace) resulted in significant NiGa phase formation but cooling slowly at about 0.5 °C/min lead to phase pure Ni_5Ga_3. After synthesis, the intermetallic ingot is ball milled to a powder for catalytic applications. This approach is ideally suited for the synthesis of model catalyst for studying structure-function relations since it ensures high phase

Table 1
Selected examples of intermetallic catalysts and potential advantage over pure metals.

Reaction Chemistry	Intermetallic Compound	Traditional Catalyst	Advantage
$C_2H_2 + H_2 \rightarrow C_2H_4$	PdZn [37], Ni_5Zn_{21} [38], PdIn [39], Pd_2Ga [40], PdGa [2], Pd_3Ga_7[41], $Al_{13}Fe_4$ [42].	Pd and Ni	Higher ethylene selectivity.
$C_6H_5CCH + H_2 \rightarrow C_6H_5CHCH_2$	Ni_5Ga_3, Ni_3Ga, NiGa [43]	Pd and Ni	Higher selectivity, greater time-on-stream stability and cost benefits (w.r.t. Pd).
$C_4H_6 + H_2 \rightarrow C_4H_8$	PdSn [44], PdPb [45], Pt_3Ge [46]	Pd	Improved selectivity.
$CH_4 + CO_2 \rightarrow 2CO + 2H_2$	Co_2Hf, NiSc [47]	Ni	Improved activity and stability (decreased carbonaceous deposition).
$CO_2 + H_2 \rightarrow C_1 + C_2$	Ni_5Ga_3, NiGa, Ni_3Ga [48]	Cu	Higher activity.
$CO_2 + H_2 \rightarrow CH_3OH$	Ni_5Ga_3 [49]	Cu/ZnO	Can be operated at ambient pressure instead of 50-100 bar.
$CH_3OH + H_2O \rightarrow CO_2 + 3H_2$	PdZn [50]	Cu/ZnO	Higher resistance to sintering and higher CO_2 selectivity.
$HCOOH \rightarrow CO_2 + H_2$	PdZn [51], PtBi [52]	Pt	Higher selectivity to CO_2 compared to CO.
$C_6H_{12} \rightarrow C_6H_6 + 3H_2$	Pt_3Sn, PtGe [53]	Pt	Higher selectivity and resistance to coking.
$C_4H_{10} \rightarrow C_4H_8 + H_2$	Pt_3Sn, PtGe [53]	Pt	Higher selectivity and resistance to coking.

purity and excellent compositional control. Further, the possibility of any support effect is eliminated. However, the surface area of the catalyst is low ($\sim 1 m^2/g$, 10–50μ particles) leading to limited practical applicability [2]. Mukhopadhyay et al. [63] found that even after extensive ball milling the particle size of the Cu_5Zn_8 intermetallic could not be reduced to below 150 nm with a very large particle size distribution (Fig. 5a). Moreover, extensive ball milling may lead to sample contamination from ball material or the walls of the container. Further, the high energy, uncontrolled and non-equilibrated ball milling step may result in the deviation of surface composition from the expected bulk values. Therefore, an annealing step after ball milling is essential to restore the material to its thermodynamically preferred form.

Miura et al. [51] adapted the high temperature diffusion technique to synthesize supported Pt-Zn NPs. A Pt/Vulcan material and a lump of Zn (mole ratio 1:1) physically separated in a tube furnace were heated to 500 °C for 8 h under a flow of nitrogen. The entire amount of Zn was consumed and PtZn intermetallic NPs were synthesized with particle size less than 15 nm (Fig. 5b). This approach is limited since it could not be extended to metals such as Bi, Pb or Tl because of their lower vapor pressure (even at temperatures approaching 800 °C). Shao et al. [64] mixed together stoichiometric amount of Ni and Mg NPs formed by arc melting and heated to 623 K under hydrogen atmosphere for 2 h leading to the formation of Mg_2NiH_4 which can be dehydrogenated to phase pure Mg_2Ni (d = 30–50 nm) by evacuation at 623 K for 45 min.

Li et al. [43] used *in situ* reduction of layered double hydroxide precursor and found that the starting composition as well as the reduction temperature had an effect on the synthesized Ni-Ga intermetallic phase and particle size. Zhou et al. synthesized a PdZn intermetallic by calcining and reducing a Pd/ZnO material [37]. An identical method was also successful in synthesizing NiZn/ZnO NPs [65]. Onda et al. [66] used chemical vapor deposition of a Sn complex on Ni/SiO_2 to prepare a number of phase-pure Ni-Sn supported catalysts. Milanova et al. used a template approach to synthesize Cu-Sn and Ni-Sn NPs using a porous C-foam support [67]. Solvothermal techniques have been successfully applied by Sarkar et al. [68] to synthesize Pd_2Ga. Other possible techniques include electrodeposition [69] and mechanical attrition methods (reviewed in detail by Koch and Whittenberger [70]). Several techniques have also been applied to access meta-stable ordered intermetallic structures (which are not accessible through high temperature bulk synthesis) but phase-purity is often an issue due to the presence of residual pure metals or oxides [71–73].

Researchers have also tried to adopt established wet chemical methods for the synthesis of monometallic NP to intermetallics. Cable and Schaak synthesized a number of M-Zn intermetallics through a solution synthesis method starting with a zero-valent organometallic Zn source [74]. Notable amongst these is the Cu_5Zn_8 γ-brass phase because accessing this phase in NP dimensions (Fig. 5c) is challenging owing to its large and complex but highly symmetric crystal structure. Cable and Schaak developed a modified polyol method for the synthesis of M-Sn and Pt-M' intermetallics with sizes ranging from 10 to 100 nm [75]. Other similar solution based techniques are also reported in literature [39,76–79]. Brian et al.[80] synthesized ternary intermetallic Au-Cu-Sn and Au-Ni-Sn phases through polyol method. A major drawback of many of these techniques is that there is no rational guideline as to which starting composition is required to access which intermetallic phase (Table 2). Further, in many solution-based synthesis of intermetallics [74,75], rigorous particle size control has also proven to be elusive. Zn is known to form a large number of catalytically relevant intermetallic compounds (see Section 4) [38,81]. However, a potential drawback of Zn containing intermetallics is the ubiquitous presence of ZnO (observed by Schaak, [74] Miura [51] and others [65,82]) which may significantly affect catalytic properties [65]. Barkholtz et al. [83] circumvented this issue by using LiOH (at 200°C), a reducing agent, as the synthetic medium to synthesize PdZn.

Recently, significant effort has been focused on synthesizing hybrid intermetallics-pure metal/alloy catalysts with specific core-shell architecture via various de-alloying techniques. Examples are available in literature where either the core or the shell or even both may be intermetallics [84–88]. These materials are of particular importance for catalyzing electrochemical half reactions commonly utilized in fuel cells, as discussed in Section 4.

In general, simply ensuring stoichiometric addition of different metal precursors is neither a sufficient nor a necessary condition for intermetallic NP synthesis. Proper characterization is essential to ascertain that the correct phase is indeed formed and preclude the existence of mixed phases, undesired oxides or core-shell structures.

3. Characterization of intermetallic catalysts

The primary purpose of this section is to highlight that many characterization techniques are more informative in case of intermetallics than monometallic catalysts and multiple techniques should be considered during the characterization of intermetallic catalysts. The approach for characterizing alloys and intermetallics are identical. However, for alloys, all values are averaged over the entire loading but for intermetallics (because of long range ordering) the values may be considered to hold for each individual unit cell and not a statistical average over millions of unit cells. Apart from the methods discussed herein other methods that are used for monometallic catalyst characterization should also be performed for intermetallic catalysts. These include Brunauer-Emmett-Teller (BET) surface area, temperature programmed reduction, oxidation and desorption and elemental analysis.

3.1. Diffraction methods

Diffraction (most commonly X-ray diffraction) is the initial characterization technique performed on a newly synthesized material. It often (particle size typically > 20 nm) provides conclusive evidence

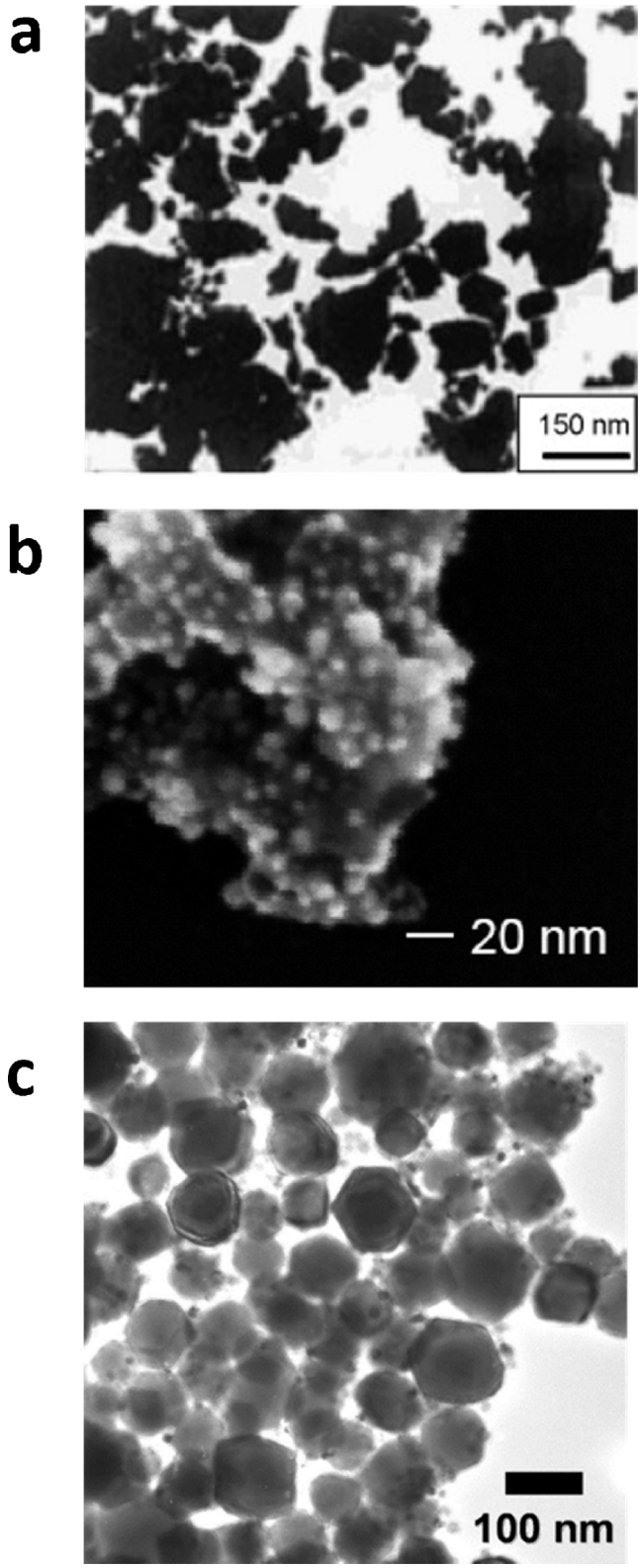

Fig. 5. (a) Cu_5Zn_8 after ball milling bulk ingots for 40 h;(reprinted with permission from reference [63], copyright 2007, Elsevier.) (b) PtZn/Vulcan catalysts by Zn vapor diffusion (reprinted with permission from reference [51], copyright 2009, American Chemical Society) and (c) Cu_5Zn_8 by solution synthesis (reprinted with permission from reference [74], copyright 2007, American Chemical Society).

Table 2
Compilation of starting and final metal composition during synthesis of intermetallic particles through solution based techniques.

Product Composition	Initial Composition	Reference
Pd:Ga = 2:1	Pd:Ga = 2.5:30	Ota et al. [40]
Pt:Sn = 1:4	Pt:Sn = 1:9	Downing et al. [76]
Ir:Sn = 3:7	Ir:Sn = 2:9	Downing et al. [76]
Ni:Sn = 2.7:2	Ni:Sn = 3:4	Yakymovych and Ipser [77]
Cu:Sn = 1:1	Cu:Sn = 6:5	Milanova et al. [67]
Pd:Zn = 1:1	Pd:Zn = 49.2:465	Cable and Schaak [74]
Cu:Zn = 5:8	Cu:Zn = 50:412	Cable and Schaak [74]
Au:Zn = 1:1	Au:Zn = 50:619	Cable and Schaak [74]
Au:Zn = 3:1	Au:Zn = 53:206	Cable and Schaak [74]
Ag:Sn = 4:1	Ag:Sn = 1:1	Cable and Schaak [75]
Au:Sn = 5:1	Au:Sn = 1:1	Cable and Schaak [75]
Fe:Sn = 1:2	Fe:Sn = 1:5.9	Cable and Schaak [75]
Ni:Sn = 3:4	Ni:Sn = 1:4.4	Cable and Schaak [75]
Pt:Sn = 1:1	Pt:Sn = 1:4.3	Bauer et al. [89]
Pt:Pb = 1:1	Pt:Pb = 1:1.1	Bauer et al. [89]
Fe:Pt = 1:3	Fe:Pt = 0.5:1.1	Bauer et al. [89]
Au:Cu = 1:1	Au:Cu = 3.1:1	Sra et al. [90]
Pt:Pb = 1:1	Pt:Pb = 1:1	Alden et al. [91]
Pd:Sn = 1:1	Pd:Sn = 1:1.6	Chou and Schaak [92]
Fe:Sn = 1:2	Fe:Sn = 1:2.1	Chou and Schaak [92]
Ni:Sn = 1:3	Ni:Sn = 1:3.3	Chou and Schaak [92]

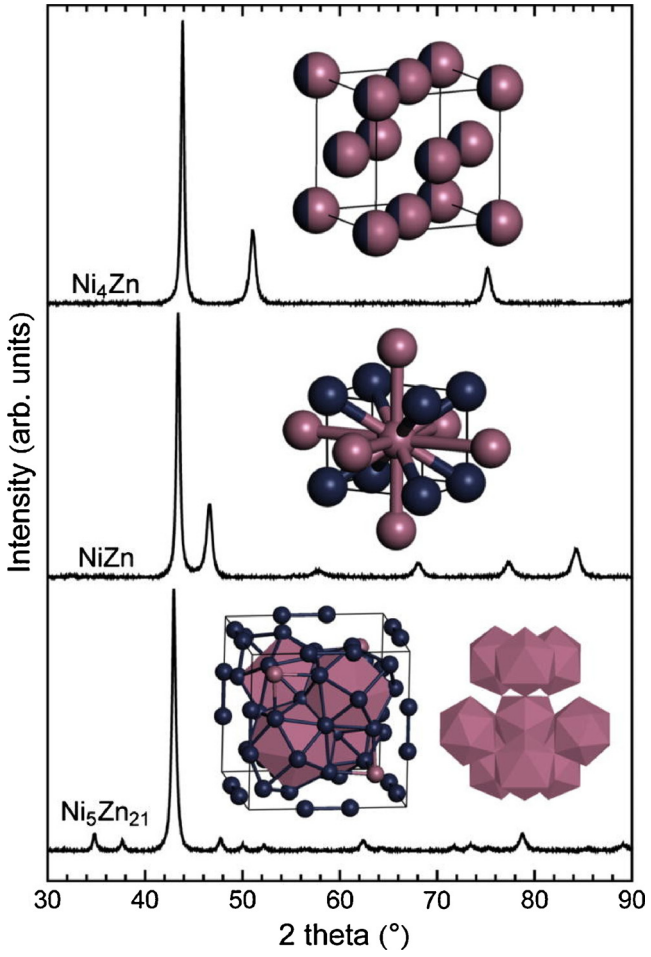

Fig. 6. XRD patterns and crystal structure of different Ni-Zn alloy (Ni_4Zn) and intermetallic (NiZn and Ni_5Zn_{21}) phases. Materials synthesized through bulk synthesis followed by ball-milling. Reprinted with permission from reference [38], copyright 2014, Elsevier.

towards phase identity and corresponding purity and the general success of the synthesis as most intermetallic compounds' diffractograms differ significantly from the constituent pure metals (owing to large difference in crystal structures, Fig. 6). Quantitative X-ray or neutron diffraction accompanied by Rietveld refinement [93] (or other techniques)[94,95] of the diffraction data may also provide insight into the atomic site occupation in the crystal lattice [4,62,96] and valuable hints towards active site morphology. For example, using Rietveld refinement of neutron diffractogram, Spanjers et al. [96] identified that in the Ni_8Zn_{44} γ-brass phase all Ni atoms are completely isolated in Zn matrix which leads to the conclusion that barring any major surface segregation effects (to be discussed in detail; general guidelines for predicting surface segregation tendencies of many metal pairs is available in literature [97,98]) Ni_8Zn_{44} will form a single atom hydrogenation catalyst.

For ternary phases a simultaneous refinement of X-ray and neutron diffractograms is expected to provide the best results for determining site occupation factors [99]. However, for many ternary intermetallic systems using either neutron or X-ray diffraction is found to be sufficient depending on the respective diffraction cross-sections of the constituent elements for the different probes [4,100–102].

Electron diffraction can also be applied to identify the formation of intermetallic phases. This method is particularly suited for small NPs (< 10 nm). The signal for electron diffraction is much stronger than for X-ray or neutron diffraction and hence sufficient signal is obtained for electron diffraction even when X-ray or neutron diffractograms show poorly resolved, low intensity, or broad peaks. However, electron diffraction can in general only be performed on a finite number of particles (as opposed to powder diffraction) and therefore is less effective in confirming phase purity of the entire sample. Details of this technique is reviewed elsewhere [103].

3.2. TEM (transmission electron microscopy) & STEM (scanning transmission electron microscopy) or SEM (scanning electron microscopy)-EDS (energy dispersive x-ray spectroscopy)

TEM and STEM-EDS are powerful techniques for characterizing multi-component NPs (beyond simple particle size distribution) and provide supporting data to the diffraction analysis. Diffraction techniques are dependent on the crystallite volume and heavily biased towards the phase having the larger crystallites while making it extremely difficult to detect highly dispersed or amorphous secondary phases. For example, an envelope of Na or Zn hydroxide or oxide was detected by Miura et al. [51] during TEM imaging of PtZn particles even though no such peaks were present in the X-ray diffractograms. STEM-EDS provides additional information regarding the composition of each individual NP. For example, while XRD can only predict if the bimetallic is single phase, complimentary STEM-EDS elemental mapping can confirm if the metal ratio of each individual NP is also identical or varies within the compositional bounds of the corresponding phase. Variation of the metal ratio even within the same phase may lead to critical differences in active site morphologies. Further, elemental mapping through STEM or SEM-EDS (depending on particle size) can provide visual conformation of alloying.

3.3. EXAFS (extended x-ray absorption fine strucutre)

EXAFS is a method which finds application in bi-metallic systems to identify the average coordination geometry (and interatomic distances) of each kind of atom. In case of NPs, EXAFS can provide insight regarding the extent of site isolation which is an important consideration (geometric effect) for designing selective intermetallic catalysts. For example, Feng et al. [39] explained the superiority of PdIn over Pd_3In for acetylene semi-hydrogenation on the basis of the higher Pd-In coordination (5.7 ± 1.2) in the former compared to Pd_3In (4.0 ± 1.7) which indicated a higher degree of Pd isolation, inhibiting over-hydrogenation and oligomerization pathways. Childers et al. [81] have shown that the catalytic activity for neopentane hydrogenolysis decreases as the average Pd-Zn coordination number increases in the catalyst and becomes zero when it is 5.2.

3.4. HS-LEIS (high sensitivity-low energy ion spectroscopy) and other surface sensitive techniques

HS-LEIS is a relatively new method and its technical details are reviewed elsewhere [104,105]. The salient point of LEIS is that it uses a beam of very low energy (3–5 keV) noble gas ions (He^+ or Ne^+) to probe only the top monolayer of the material, making it truly surface sensitive compared to traditional surface quantification techniques like X-ray photoelectron spectroscopy (XPS, typical penetration depth ~10 nm) and Auger Electron Spectroscopy (AES). Since catalysis is a surface phenomenon, LEIS is an ideal tool to verify the surface composition (which may prove to be different than bulk composition). Depth profiling is possible through sputtering by Ar^+ and sequentially removing a desired number of monolayers from the top. Such depth profiling can provide a clear understanding of surface segregation effects, that is the composition in each subsequent layer should approach (and ultimately saturate at) the bulk composition (estimated through ICP or EDS). LEIS is often used together with a more traditional surface characterization technique like XPS or AES which have higher penetration depths. A clear difference in signal between AES and LEIS is presented by Stadlmayr et al. [106] (Fig. 7a) for a Pd-Zn near-surface intermetallic (Fig. 7b) on a Pd substrate. This study highlights the complementarity between methods since in conjunction they provide a more complete description of atomic segregation than either method alone.

Rameshan's study on near-surface intermetallic PdZn (formed by depositing Zn on a Pd foil followed by annealing) for catalytic steam reforming of methanol [107] had led to a surprising conclusion that the relative selectivity between CO and CO_2 completely reversed at ~600 K (see Fig. 12 in Section 4 for reaction data). Stadlmayr et al. [106] explained this phenomenon by demonstrating that as the temperature increases above 600 K, the top surface Zn concentration starts to decrease (LEIS signal) but not as significantly as the sub-surface Zn concentration (AES signal). This indicates Zn depletion is much faster in the subsurface than the surface so that the catalyst is virtually an intermetallic/alloy monolayer on a Pd substrate at ~650 K. Fig. 7b provides a schematic of this temperature dependent transformation. The presence of only Pd in the first subsurface layer strongly affects the surface corrugation (relative heights (normal to the facet) of Zn and Pd centers at the top surface) which influences the observed selectivity [108–110].

Rameshan [111] has used LEIS and XPS techniques to show that a near surface PdGa intermetallic may be synthesized by depositing a controlled amount Ga on a Pd foil followed by annealing. Kopfle et al. [112] has also used LEIS and XPS to conclude that under reductive conditions only Pd is present on the surface of a Pd-Zr intermetallic but under dry methane reforming conditions Zr is exposed on the surface. The presence of Zr on the surface was determined as a key factor for high catalytic reactivity.

3.5. Chemisorption + calorimetry

Chemisorption is a powerful tool for catalyst characterization and for the estimation of the number of active sites exposed to a potential reactant. In case of an intermetallic, due to the unique surface morphology as well as potential surface segregation effects, determining the true number of active sites becomes a significant challenge that may be solved via chemisorption. The ability to perform calorimetric measurements in conjunction with chemisorption provides further insight into the chemical nature of the active sites and their geometric/electronic distinction from the pure metals (as mentioned before, varying the interaction between catalyst and reactant is a major motivation for

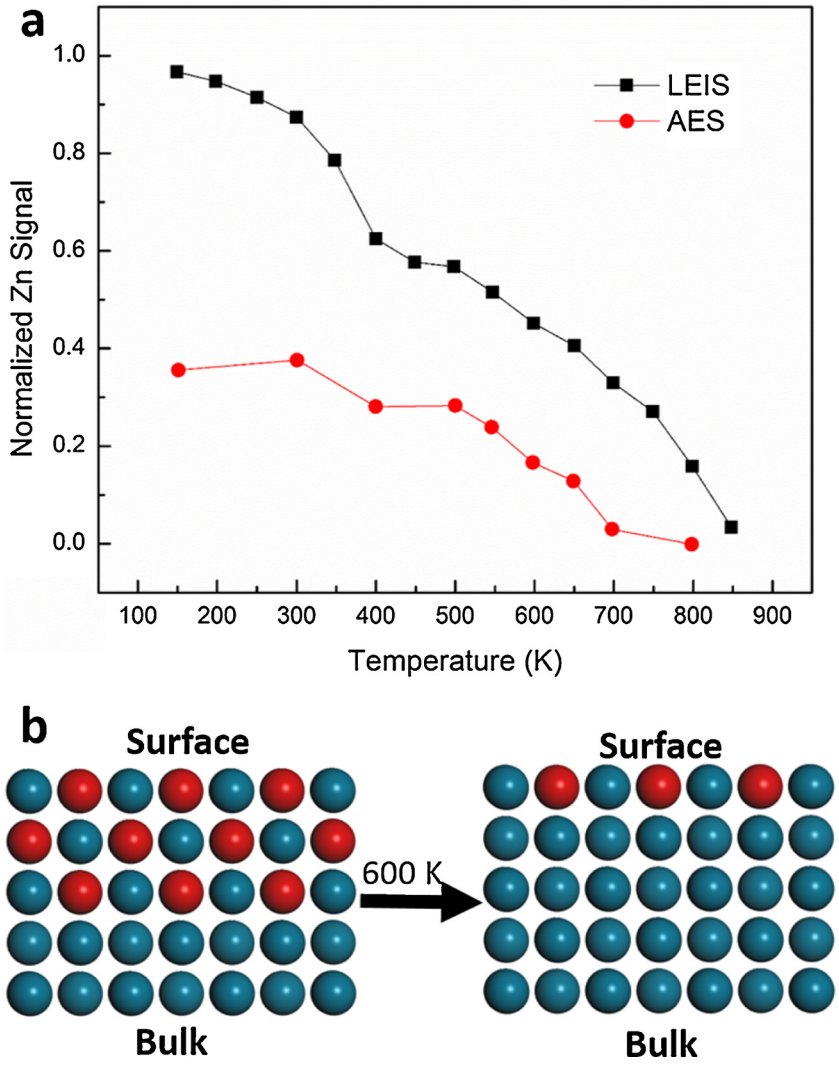

Fig. 7. (a) AES and LEIS determined Zn composition of a PdZn near-surface intermetallic on a Pd substrate (re-plotted with permission from reference [106], copyright 2010, American Chemical Society). (b) Schematic representation of the conversion of multi-layer near-surface intermetallic to a mono-layer top-surface intermetallic at ~600 K. Blue spheres represent Pd and red Zn (For interpretation of the references to colour in this figure legend, the reader is referred to the web version of this article).

intermetallic selective catalyst design). Zhou et al. [37] reported (Fig. 8) that the heat of adsorption of hydrogen on PdZn intermetallic NPs is about 40 kJ/mole lower than on pure Pd NPs at low coverage and the discrepancy is even higher as the coverage (specific uptake) is increased. The sharper decrease in adsorption energy for equivalent coverage may also possibly hint at fewer number of sites (leading to greater steric repulsion) in the PdZn intermetallic compared to pure Pd.

In an earlier work by Vannice and co-workers, detailed methods are described for quantifying the surface composition (number of Cu and Pt atoms exposed on average) of a representative bimetallic catalyst where both metals are of catalytic relevance (Cu-Pt) [113]. This method involves a number of successive surface oxidation and titration steps using CO as adsorbate and N_2O as the oxidizing agent because of its ability to preferentially convert surface Cu(0) to Cu(I). The presence of Cu(I) is critical because it possesses CO chemisorption ability (in contrast to Cu(0) or Cu(II)) and provides a method to estimate total metal surface atoms (as Pt also chemisorbs CO). The number of Pt atoms are identified via CO chemisorption of the reduced catalyst (Cu(0) does not chemisorb CO) and the number of Cu surface atoms is identified by subtraction of Pt surface atoms (CO chemisorption on reduced sample) from the total number of surface atoms (CO chemisorption on partially oxidized sample). This method can not only be extended to phase pure intermetallics but can in fact provide greater insight because of the structural homogeneity (in terms of active site morphology) of the intermetallic.

3.6. CO-FTIR (fourier transform infra-red) spectroscopy

CO-FTIR spectroscopy is another technique which can be applicable in case of specific (particularly Pd-containing) intermetallics. For single atom Pd sites, CO can only bind in an atop position (linear configuration, Pd−CO) whereas for a site with Pd-Pd coordination, CO also has the opportunity to bind in bridge position (Pd−CO-Pd). The vibration frequency for these cases can be distinguished by FTIR (peak at ~2050 cm^{-1} for atop and at ~1900 cm^{-1} for bridge) and help to determine the extent of site isolation (single atom versus multi-atom).[2] Fig. 9 demonstrates monometallic Pd nano-particles can support both linear and bridge bonded CO by virtue of its Pd-Pd coordination, while isolated Pd atoms in the Zn matrix of a PdZn intermetallic nanoparticle can only support linearly bonded CO (demonstrated by a single peak at 2050 cm^{-1}).

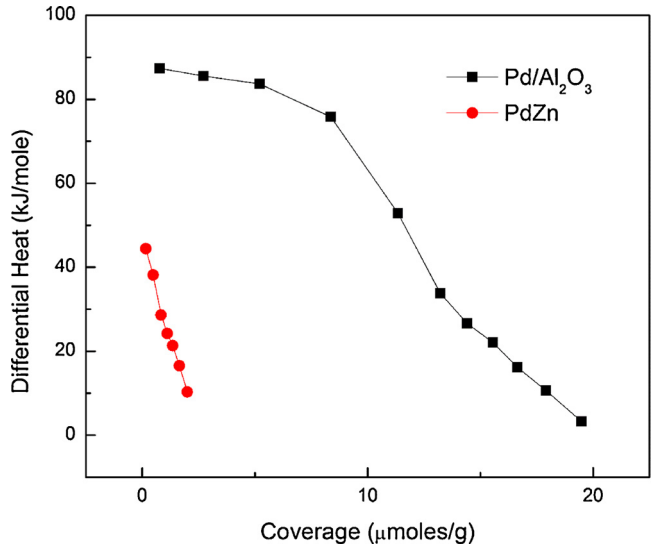

Fig. 8. Heat of adsorption of hydrogen on Pd and PdZn intermetallic catalysts. Reprinted with permission from reference [37], copyright 2016, American Chemical Society.

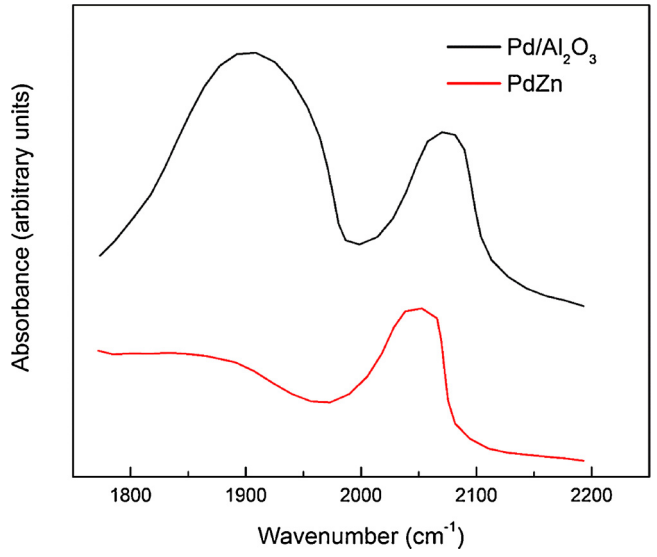

Fig. 9. CO-FTIR spectroscopy on Pd/Al_2O_3 and PdZn NPs. Reprinted with permission from reference [37], copyright 2016, American Chemical Society.

3.7. Probe reactions and DFT

Despite the wide range of bulk and surface sensitive techniques available there is no way to probe the chemical morphology of the exposed surface. While LEIS or well-designed chemisorption experiments can provide estimates regarding the chemical composition of the surface, they allow no understanding of the coordination geometry of the different atoms exposed on the surface (which may turn out to be different from the bulk due to surface segregation effects). The easiest way to access such insight is through a combination of probe reactions and DFT as detailed by Spanjers et al. for the Ni-Zn γ-brass phase [96]. It was determined through Rietveld refinement and DFT calculations the Ni-Zn γ-brass phase crystal lattice contained isolated Ni active atoms at 15.4 at% Ni but Ni-Ni coordination (Ni-Ni-Ni trimer site) appeared when the Ni concentration exceeded 15.4 at% (Ni_8Zn_{44}) by Zn replacement (in particular Ni_9Zn_{43} and $Ni_{10}Zn_{42}$, see Fig. 10). However, H_2-D_2 exchange and ethylene hydrogenation barriers showed this increase in Ni-Ni coordination in the lattice had no effect on catalysis implying that only isolated Ni atoms are expected to be exposed irrespective of Ni concentration. This hypothesis was confirmed by DFT surface energy calculation and Wulff construction where it was shown single atom Ni active sites were more favorable to be exposed than Ni-Ni-Ni trimer active sites (Fig. 10).

An ideal probe reaction should be one whose kinetics is well-documented on appropriate reference material and the reaction network is predictable and relatively simple to analyze. Common probe reactions are H_2-D_2 exchange, ethylene and benzene hydrogenation and ethane hydrogenolysis amongst others [54,65,114–118]. Of course, the actual choice of probe reaction depends on the desired catalytic propensities to be investigated (for example, hydrogen or carbon bond cleavage ability).

4. Intermetallics in catalysis – survey of results from the literature

Schwab was the first to recognize anomalous activation barriers in case of unsupported alloy and intermetallic catalysts compared to their pure metal constituents [24] and studied the effect of compositional variation within the same phase as well as between different crystallographic phases for formic acid dehydrogenation (discussed below) as early as 1946. Since the late 1980 s the interest in intermetallic catalysts has garnered significantly more attention and efforts with increased commercial incentive of synthesizing low cost and high performing catalysts. Here we present some common classes of reactions for which intermetallics have significantly superior performance than pure metals.

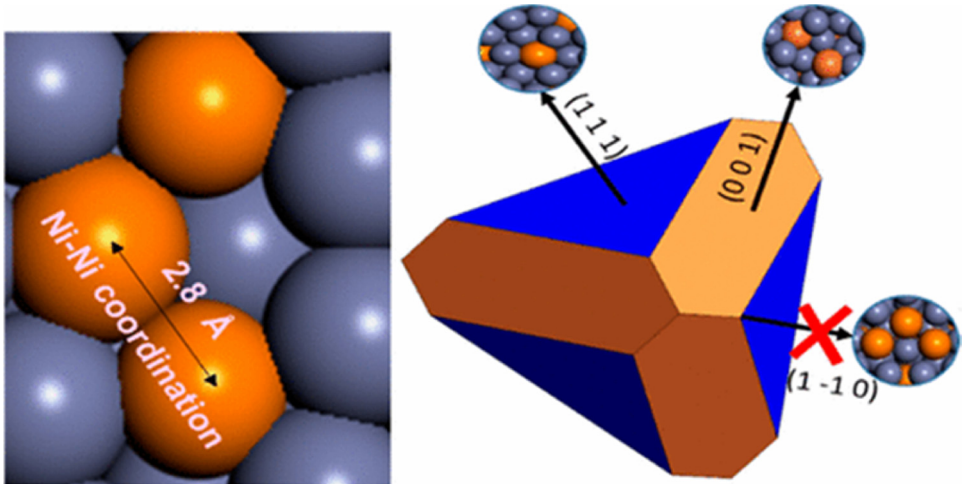

Fig. 10. (left) Ni-Ni-Ni trimer present in the bulk of Ni_9Zn_{43} as determined by Rietveld refinement of Neutron diffraction patterns and (right) the corresponding Wulff Construction showing the trimer containing (1–1 0) facet is not energetically favored to be exposed. The inlays in (right) demonstrate the respective surface terminations for the different facets considered. Orange spheres represent Ni and grey spheres Zn. Reprinted with permission from reference [96], copyright 2017, American Chemical Society.

4.1. Formic acid dehydrogenation

Formic acid dehydrogenation is a popular model reaction because of the simple nature of the substrate as well as its practical importance in modern fuel cell operation. Schwab et al. initially studied the activation barrier for this model system (on a large number of Ag-M and Au-M' catalysts) and determined different Hume-Rothery phases had markedly different activation energies. It was determined to be an electronic effect (establishing the applicability of Hume-Rothery's *vec* concept in catalysis) as the barrier was strongly correlated with intrinsic properties commonly associated with the valence shell electronic configuration of metals, such as electrical resistivity and hardness [119,120]. More recently, it has been found that the selectivity of formic acid dehydrogenation is also an important consideration since the formation of CO (as by-product) can poison typical fuel cell catalysts such as Pt. This has prompted the development of intermetallic catalysts which are less susceptible to CO poisoning than Pt. PtBi is suggested to be a suitable alternative demonstrating high activity (due to electronic effects) and low CO adsorption energies (increased Pt-Pt distance compared to pure Pt) [52,121]. Similar results were also observed for Pt-Zn and Pt-Pb intermetallics [51,122,123].

4.2. Selective alkyne semi-hydrogenation

Selective semi-hydrogenation of alkyne in an alkene rich stream is a commercially important and widely studied chemistry. Alkynes are typically present in trace amounts in alkene feeds destined for polymerization (a multi-hundred-billion-dollar industry) [124]. However, alkynes are poisonous to the polymerization catalyst and must be reduced to ppm level. Ideally, only the alkyne should be selectively semi-hydrogenated to decrease its concentration and enhance the alkene feed stream. However, typical hydrogenation catalysts either lead to total hydrogenation of all unsaturated C—C bonds to (low value) alkane (Pd) or forms oligomers and green oil (Ni).

The geometric (and possibly also the electronic) effects of alloying is seen to impart suitable catalytic properties for this reaction to a large number of intermetallic compounds. In this case, the primary design concept is limiting Pd cluster size to just a few atoms as alkyne semi-hydrogenation requires fewer number of Pd atoms than any of the competing steps [125,126]. It is important to note that reducing the number of Pd atoms per active site (by adding inactive metals as spacers) to increase selectivity is always associated with a loss in activity and identifying the best catalyst is essentially an optimization challenge, balancing the gain in selectivity with the loss in activity [127].

Of all alkyne semi-hydrogenation reactions, acetylene semi-hydrogenation is considered to be the most challenging (in terms of selectivity) because of the small molecular size and very strong interaction of reaction intermediates with transition metal surfaces (particularly Pd) [128]. Several intermetallics such as Pd-In, [39] Pd-Zn [37] and Pd-Ga [2,40,41,129] have shown high selectivity (sometimes > 90%) for this reaction.

The current focus in this field is replacing Pd with cheaper base metals. Spanjers et al. [38] studied the Ni-Zn phase diagram and found that only the γ-brass phase has a sufficiently high selectivity (~65%), almost 3 times higher than any other Ni-Zn alloy (Fig. 11). This was attributed to the high degree of site isolation of Ni in Zn due to the unique crystal structure of this phase. In fact it was concluded that the γ-brass phase had effectively single atom Ni active sites [96] which led to high ethylene selectivity by minimizing oligomerization. Liu et al. [130] has demonstrated high acetylene semi-hydrogenation selectivity on Ni_3Ga and Ni_3Sn_2. Another highly selective Al-Fe catalyst having a unit cell of more than 100 atoms has been reported by Armbruster and co-workers [42]. It was found that neither of the pure components under experimental conditions was able to catalyze the reaction. The catalytic activity was therefore attributed to the small but apparently

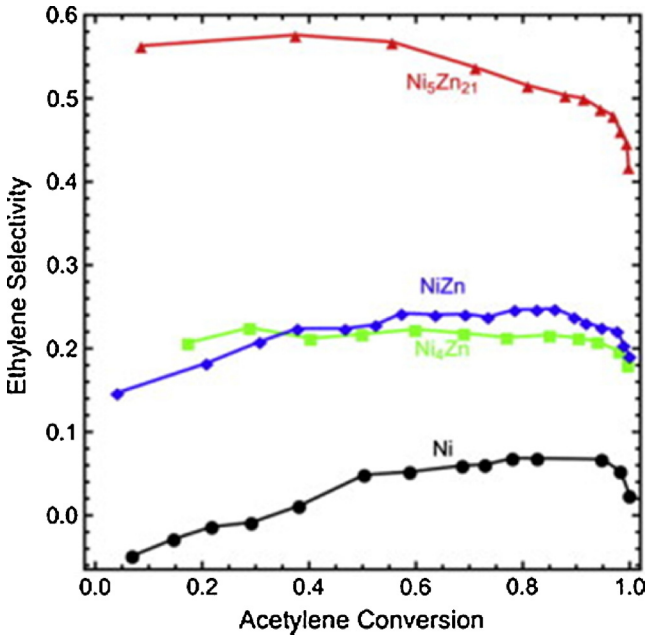

Fig. 11. Acetylene semi-hydrogenation selectivity of different Ni-Zn alloy (Ni_4Zn) and intermetallics (NiZn and Ni_5Zn_{21}) at 160 °C and initial composition of 2.5 torr C_2H_2, 27 torr H_2, 53 torr C_2H_4 and balance He. (Reprinted with permission from reference [38], copyright 2014, Elsevier).

significant change in DOS due to alloying. Further, reduction of Fe-Fe coordination was also hypothesized to be an important factor for reducing oligomerization.

Intermetallic compounds have been found to be effective for semi-hydrogenation of higher molecular weight alkynes as well. For example, Ni-Ga intermetallics were found to be selective for phenylacetylene semi-hydrogenation [43,130] while Pd_3Pb is selective for hydrogenating functionalized alkynes (aldehyde, ketone, carboxylic acid and ester) to (E)-alkenes [131].

4.3. Steam reforming of methanol

Steam reforming of methanol is gaining popularity in the field of fuel cell development because methanol can act as a relatively safe, high yield and easy to handle liquid source of hydrogen. However, parallel CO formation pathways must be suppressed to ensure the success of any methanol based hydrogen storage approach. Pure Pd and Pt are exclusively selective to CO and is therefore not suitable. On the other hand, near-surface intermetallics such as Pd-Zn, Pd-Ga and Pd-In which are generated *in situ* from Pd/MO_x materials under reactive or pretreatment conditions are found to be highly selective towards the desired products ($CO_2 + H_2$). The high selectivity is attributed to the different preferred configurations of HCHO (which is a key intermediate) on intermetallic versus pure metal surfaces possibly due to differences in electronic structure [132]. Of these PdZn is perhaps the most widely studied; Armbruster et al. has published a detailed review of this chemistry on PdZn catalysts [50]. As pointed out in Section 3, the near-surface composition plays a huge role in the selectivity of PdZn catalysts for this chemistry. Rameshan et al. reported that if the intermetallic existed to a depth of at least 5 layers below the surface (including the top exposed surface) the catalyst is selective towards CO_2 but if there is only a surface monolayer of the intermetallic on a Pd substrate then the pathway for CO production is favored [107].Further, as previously mentioned (refer Section 3 and Stadlmayr et al. [106]), the thickness (number of layers from the surface) of PdZn near-surface intermetallic is a function of temperature and becomes effectively a monolayer (on a Pd substrate) above 623 K thereby reversing the CO/

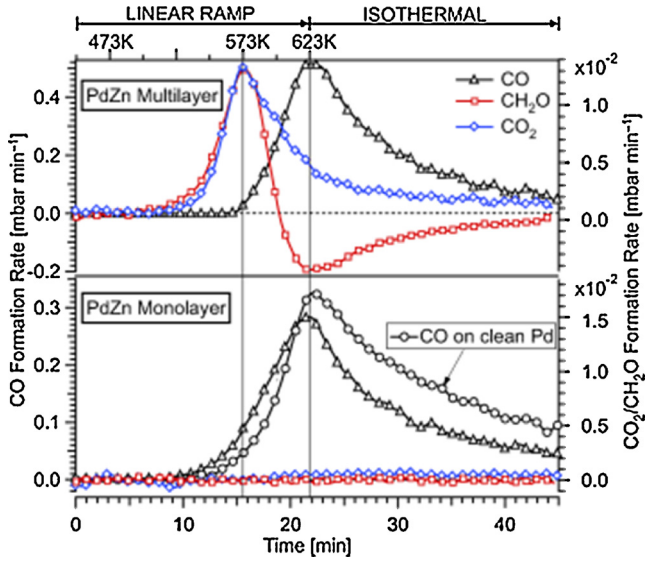

Fig. 12. Temperature programmed methanol steam reforming (12 mbar methanol, 24 mbar water and 977 mbar He).(Reprinted with permission from ref [107], copyright 2010, Wiley-VCH).

CO_2 selectivity. This phenomena is represented in Fig. 12.

4.4. Low temperature electrocatalytic oxygen reduction

The electrocatalytic reduction of oxygen is the typical cathode half reaction for low temperature (polymer-electrolyte-membrane, phosphoric acid, direct alcohol etc.) fuel cells. The preferred pure metal catalyst for this reaction is Pt. However, the very high cost of Pt is detrimental to the commercialization of this clean energy technology and there is considerable focus on increasing the intrinsic activity (on a per mole Pt basis) through alloying with base metals and introducing beneficial active site ensemble effects [133–135]. The key descriptor for activity is the adsorption energy of oxygenated species (most importantly OH) on the catalyst surface. Reduction in the OH bond strength is positively correlated with catalyst activity [136]. Alloying of Pt with suitable and much cheaper transition metals (Fe [137–139], Cr [140,141], Co [142], Ni [143]) leads to a Pt d-band downshift which weakens this surface – OH interaction, thus increasing activity [144]. Further, it is seen that the specific activity of intermetallic Pt-M phases are always higher than alloys of similar composition [145]. Even though the exact reason behind this observation is not yet known, one possibility certainly may be that the disorder in random alloys only results in a fraction of the active sites to have the desired ensemble morphology (as determined by stoichiometry) whereas in the ordered intermetallics the desired ensemble morphology is guaranteed in the entire catalyst bed. In recent times several research groups have focused on strategic design of hybrid core-shell intermetallic catalysts which show some of the highest oxygen reduction activity and time-on-stream stability reported to date [85–87].

4.5. Other examples

Several other chemistries have also been successfully tested on different intermetallic materials. For example, Ni-Ga intermetallics are reported to be highly active and selective catalysts for CO_2 reduction to methanol [49] and even to alkanes and alkenes [48]. Pt-Ge, Al-Cu and Pd-Zn intermetallic catalysts were found to be selective for butadiene semi-hydrogenation [46,146]. Pd-Zr and Co-Hf intermetallic compounds are seen to be more active for dry reforming of methane compared to the constituent pure metals [47,112]. Takeshita et al. has reported a number of transition metal-rare earth metal intermetallics to be highly active for ammonia synthesis [147]. Pd-Zn catalysts have been found to be effective for a variety of reactions (beyond those mentioned above) including partial methanol oxidation, methanol dehydrogenation and ester hydrogenation [148–150].

5. Conclusions and future outlook

In addition to the catalytic reactions mentioned above, intermetallics, by virtue of their unique properties (compared to pure metals) may be effectively employed to perform a large number of chemical transformation (see reviews by Furukawa and Komatsu [151,152] for more examples) while providing added opportunities for optimizing activity and selectivity through manipulation of active site nuclearity and electronic structure. In this context it is worth mentioning that catalytic studies on ternary (or higher) intermetallic phases are rarely reported as of yet even though polymetallic catalysts (typically involving doping of small amounts of one or more metal as modifier) have been reported in literature [153–155]. This paper has highlighted the challenges of reliably synthesizing phase-pure intermetallic NPs. It is expected that synthesizing ternary phases or intermetallics with catalytically enhanced special nano-porous structures will be even more challenging. However, such efforts have already gained considerable focus in the last few years [80,156–159] and with the development of appropriate synthetic methods, we can potentially access an unlimited number of well-defined unique active site morphologies which may cater to any number of practically important reactions and be individually tailored for optimal performance for any type of chemistry.

Apart from better control over synthesis of intermetallics (particularly in NP form) the other significant improvement desirable in this field is to develop more sensitive and advanced methods for identifying the true surface morphology of intermetallics under reactive conditions. At present most catalytic properties of intermetallics are interpreted on the basis of bulk structure but as highlighted in this review it may prove to be a gross misinterpretation/simplification due to surface segregation effects.

Overall, it is apparent intermetallics offer several advantages over pure metals and even alloys for catalysis and will continue to gain traction in the catalysis community as we head towards a greener future where high selectivity would become indispensable to meet ever stricter waste (byproduct) disposal and raw material procurment (such as mining of crude oil) laws. Further it may be hoped that development in the areas mentioned above will not only increase our ability to synthesize optimized catalysts but also improve our understanding of the fundamental surface phenomena which effects such increased activity and selectivity, ultimately leading to enrichment of the entire field of catalysis in general.

Acknowledgements

The authors (A. D. and R. M. R.) acknowledge the US National Science Foundation (NSF grant # CBET – 1748365) for financial support of this work.

References

[1] G. Gleig, Encylopaedia Britannica, Wentworth Press, 2016.
[2] K. Kovnir, M. Armbrüster, D. Teschner, T.V. Venkov, F.C. Jentoft, A. Knop-Gericke, Y. Grin, R. Schlögl, A new approach to well-defined, stable and site-isolated catalysts, Sci. Technol. Adv. Mater. 8 (2007) 420–427.
[3] H. Okamoto, Phase Diagrams of Binary Alloys, ASM International, 2010.
[4] S. Thimmaiah, N.A. Crumpton, G.J. Miller, Crystal structures and stabilities of γ- and γ′-brass phases in Pd2–xAuxZn11 (x = 0.2–0.8): vacancies vs. valence electron concentration, Zeitschrift für anorganische und allgemeine Chemie 637 (2011) 1992–1999.
[5] F. Jona, P.M. Marcus, A first-principles study of the hume-rothery electron compounds, J. Phys. Condens. Matter 14 (2002) 1275.
[6] R. Evans, P. Lloyd, M. Rahman, On the origin of the Hume-Rothery rules for phase stability in α and β brasses, J. Phys. F: Metal Phys. 9 (1979) 1939.
[7] V.F. Degtyareva, O. Degtyareva, M.K. Sakharov, N.I. Novokhatskaya, P. Dera,

H.K. Mao, R.J. Hemley, Stability of Hume-Rothery phases in Cu–Zn alloys at pressures up to 50 GPa, J. Phys. Condens. Matter 17 (2005) 7955.
[8] G.P. Vassilev, T. Gomez-Acebo, J.-C. Tedenac, Thermodynamic optimization of the Ni-Zn system, J. Phase Equilib. 21 (2000) 287–301.
[9] I. Karakaya, W.T. Thompson, The ag – pd (silver-palladium) system, Bull. Alloy Phase Diagr. 9 (1988) 237–243.
[10] A.J. McAllster, The Al – As (aluminum-arsenic) system, Bull. Alloy Phase Diagr. 5 (1984) 577–579.
[11] D. Yardimci, P. Serna, B.C. Gates, Tuning catalytic selectivity: zeolite- and magnesium oxide-supported molecular rhodium catalysts for hydrogenation of 1,3-butadiene, ACS Catal. 2 (2012) 2100–2113.
[12] A.J. McCue, C.J. McRitchie, A.M. Shepherd, J.A. Anderson, Cu/Al2O3 catalysts modified with Pd for selective acetylene hydrogenation, J. Catal. 319 (2014) 127–135.
[13] Q.W. Zhang, J. Li, X.X. Liu, Q.M. Zhu, Synergetic effect of Pd and Ag dispersed on Al2O3 in the selective hydrogenation of acetylene, Appl. Catal. A-Gen. 197 (2000) 221–228.
[14] D. Mei, M. Neurock, C.M. Smith, Hydrogenation of acetylene–ethylene mixtures over Pd and Pd–Ag alloys: first-principles-based kinetic Monte Carlo simulations, J. Catal. 268 (2009) 181–195.
[15] R.J. Meyer, Q. Zhang, A. Kryczka, C. Gomez, R. Todorovic, Perturbation of reactivity with geometry: how far can we go? ACS Catal. 8 (2018) 566–570.
[16] M. Andersen, A.J. Medford, J.K. Norskov, K. Reuter, Scaling-relation-based analysis of bifunctional catalysis: the case for homogeneous bimetallic alloys, ACS Catal. 7 (2017) 3960–3967.
[17] J.H. Sinfelt, Catalysis by alloys and bimetallic clusters, Acc. Chem. Res. 10 (1977) 15–20.
[18] J.K. Norskov, T. Bligaard, J. Rossmeisl, C.H. Christensen, Towards the computational design of solid catalysts, Nat. Chem. 1 (2009) 37–46.
[19] B. Hammer, J.K. Norskov, Theoretical surface science and catalysis - calculations and concepts, in: B.C. Gates, H. Knozinger (Eds.), Advances in Catalysis: Impact of Surface Science on Catalysis, vol. 45, Elsevier Academic Press Inc, San Diego, 2000, pp. 71–129.
[20] M. Krajci, J. Hafner, Surfaces of intermetallic compounds: an ab initio DFT study for B20-type AlPd, Phys. Rev. B – Condens. Matter Mater. Phys. 87 (2013) 1–15.
[21] A.J. Bradley, J. Thewlis, The structures of gamma brass, Proc. Roy. Soc. 112 (1926) 678–692.
[22] M. Friedrich, S. Villaseca, L. Szentmiklósi, D. Teschner, M. Armbrüster, Order-induced selectivity increase of $Cu_{60}Pd_{40}$ in the semi-hydrogenation of acetylene, Materials 6 (2013) 2958.
[23] M. Bonfanti, C. Diaz, M.F. Somers, G.-J. Kroes, Hydrogen dissociation on Cu(111): the influence of lattice motion. Part I, PCCP Phys. Chem. Chem. Phys. 13 (2011) 4552–4561.
[24] A.P. Tsai, S. Kameoka, K. Nozawa, M. Shimoda, Y. Ishii, Intermetallic: a pseudoelement for catalysis, Acc. Chem. Res. 50 (2017) 2879–2885.
[25] K. Nozawa, N. Endo, S. Kameoka, A. Pang Tsai, Y. Ishii, Catalytic properties dominated by electronic structures in PdZn, NiZn, and PtZn intermetallic compounds, J. Phys. Soc. Jpn. 80 (2011) 064801.
[26] A. Pang Tsai, S. Kameoka, Y. Ishii, PdZn = Cu: can an intermetallic compound replace an element? J. Phys. Soc. Jpn. 73 (2004) 3270–3273.
[27] G. Kresse, J. Furthmller, Efficiency of ab-initio total energy calculations for metals and semiconductors using a plane-wave basis set, Comp. Mater. Sci. 6 (1996) 15–50.
[28] G. Kresse, J. Furthmller, Efficient iterative schemes for ab initio total-energy calculations using a plane-wave basis set, Phys. Rev. B 54 (1996) 11169–11186.
[29] V. Demange, J. Ghanbaja, F. Machizaud, J.M. Dubois, About gamma-brass phases in the Al–Cr–Fe system and their relationships to quasicrystals and approximants, Philos. Mag. 85 (2005) 1261–1272.
[30] Yao Jiang, Yuehui He, C.T. Liu, Review of porous intermetallic compounds by reactive synthesis of elemental powders, Intermetallics 93 (2018) 217–226, http://dx.doi.org/10.1016/j.intermet.2017.06.003 ISSN 0966-9795.
[31] L.M. Pike, I.M. Anderson, C.T. Liu, Y.A. Chang, Site occupancies, point defect concentrations, and solid solution hardening in B2 (Ni,Fe)Al, Acta Mater. 50 (2002) 3859–3879.
[32] J.A. Horton, C.T. Liu, M.L. Santella, Microstructures and mechanical-properties of Ni_3Al alloyed with iron additions, Metall. Trans. Phys. Metall. Mater. Sci. 18 (1987) 1265–1277.
[33] C.E. Deluque Toro, S. Ramos de Debiaggi, A.M. Monti, Study of cohesive, electronic and magnetic properties of the Ni–In intermetallic system, Phys. B: Condens. Matter 407 (2012) 3236–3239.
[34] M. Alizadeh, G. Mohammadi, Effect of micro-alloying chromium on the corrosion resistance of nanocrystalline nickel aluminide intermetallic produced by mechanical alloying process, Mater. Lett. 67 (2012) 148–150.
[35] N.S. Stoloff, C.T. Liu, S.C. Deevi, Emerging applications of intermetallics, Intermetallics 8 (2000) 1313–1320.
[36] N. Cinca, C.R.C. Lima, J.M. Guilemany, An overview of intermetallics research and application: status of thermal spray coatings, J. Mater. Res. Technol. 2 (2013) 75–86.
[37] H. Zhou, X. Yang, L. Li, X. Liu, Y. Huang, X. Pan, A. Wang, J. Li, T. Zhang, PdZn intermetallic nanostructure with Pd-Zn-Pd ensembles for highly active and chemoselective semi-hydrogenation of acetylene, ACS Catal. (2015) 1054–1061.
[38] C.S. Spanjers, J.T. Held, M.J. Jones, D.D. Stanley, R.S. Sim, M.J. Janik, R.M. Rioux, Zinc inclusion to heterogeneous nickel catalysts reduces oligomerization during the semi-hydrogenation of acetylene, J. Catal. 316 (2014) 164–173.
[39] Q. Feng, S. Zhao, Y. Wang, J. Dong, W. Chen, D. He, D. Wang, J. Yang, Y. Zhu, H. Zhu, L. Gu, Z. Li, Y. Liu, R. Yu, J. Li, Y. Li, Isolated single-atom Pd sites in intermetallic nanostructures: high catalytic selectivity for semihydrogenation of alkynes, J. Am. Chem. Soc. 139 (2017) 7294–7301.
[40] A. Ota, M. Armbrüster, M. Behrens, D. Rosenthal, M. Friedrich, I. Kasatkin, F. Girgsdies, W. Zhang, R. Wagner, R. Schlögl, Intermetallic compound Pd2Ga as a selective catalyst for the semi-hydrogenation of acetylene: from model to high performance systems, J. Phys. Chem. C 115 (2011) 1368–1374.
[41] M. Armbrüster, K. Kovnir, M. Behrens, D. Teschner, Y. Grin, R. Schlögl, Pd – Ga intermetallic compounds as highly selective semihydrogenation catalysts, J. Am. Chem. Soc. 132 (2010) 14745–14747.
[42] M. Armbruster, K. Kovnir, M. Friedrich, D. Teschner, G. Wowsnick, M. Hahne, P. Gille, L. Szentmiklsi, M. Feuerbacher, M. Heggen, F. Girgsdies, D. Rosenthal, R. Schlogl, Y. Grin, $Al_{13}Fe_4$ as a low-cost alternative for palladium in heterogeneous hydrogenation, Nat. Mater. 11 (2012) 690–693.
[43] C. Li, Y. Chen, S. Zhang, J. Zhou, F. Wang, S. He, M. Wei, D.G. Evans, X. Duan, Nickel-gallium intermetallic nanocrystal catalysts in the semihydrogenation of phenylacetylene, ChemCatChem 6 (2014) 824–831.
[44] S.H. Choi, J.S. Lee, XAFS study of tin modification of supported palladium catalyst for 1,3-butadiene hydrogenation in the presence of 1-butene, J. Catal. 193 (2000) 176–185.
[45] J. Goetz, M.A. Volpe, C.E. Gigola, R. Touroude, Low-loaded Pd-Pb/alpha-Al2O3 catalysts: effect of alloying in the hydrogenation of buta-1,3-diene and hydrogenation and isomerization of butenes, J. Catal. 199 (2001) 338–345.
[46] T. Komatsu, S.-i. Hyodo, T. Yashima, Catalytic properties of pt – ge intermetallic compounds in the hydrogenation of 1,3-butadiene, J. Phys. Chem. B 101 (1997) 5565–5572.
[47] T. Komatsu, T. Uezono, CO_2 refroming of methane on Ni- and Co-based intermetallic compound catalysts, J. Jpn. Pet. Inst. 48 (2005) 76–83.
[48] D.A. Torelli, S.A. Francis, J.C. Crompton, A. Javier, J.R. Thompson, B.S. Brunschwig, M.P. Soriaga, N.S. Lewis, Nickel–Gallium-catalyzed electrochemical reduction of CO2 to highly reduced products at Low overpotentials, ACS Catal. 6 (2016) 2100–2104.
[49] F. Studt, I. Sharafutdinov, F. Abild-Pedersen, C.F. Elkjær, J.S. Hummelshøj, S. Dahl, I. Chorkendorff, J.K. Nørskov, Discovery of a Ni-Ga catalyst for carbon dioxide reduction to methanol, Nat. Chem. 6 (2014) 320–324.
[50] M. Armbrüster, M. Behrens, K. Föttinger, M. Friedrich, É. Gaudry, S.K. Matam, H.R. Sharma, The intermetallic compound ZnPd and its role in methanol steam reforming, Catal. Rev. 55 (2013) 289–367.
[51] A. Miura, H. Wang, B.M. Leonard, H.D. Abruña, F.J. DiSalvo, Synthesis of intermetallic PtZn nanoparticles by reaction of Pt nanoparticles with Zn vapor and their application as fuel cell catalysts, Chem. Mater. 21 (2009) 2661–2667.
[52] E. Casado-Rivera, Z. Gál, A.C.D. Angelo, C. Lind, F.J. DiSalvo, H.D. Abruña, Electrocatalytic oxidation of formic acid at an ordered intermetallic PtBi surface, ChemPhysChem 4 (2003) 193–199.
[53] S. Furukawa, A. Tamura, K. Ozawa, T. Komatsu, Catalytic properties of Pt-based intermetallic compounds in dehydrogenation of cyclohexane and n-butane, Appl. Catal. A 469 (2014) 300–305.
[54] R.M. Rioux, H. Song, M. Grass, S. Habas, K. Niesz, J.D. Hoefelmeyer, P. Yang, G.A. Somorjai, Monodisperse Pt nanoparticles with well-defined surface structure: synthesis, characterization catalytic properties and future prospects, Top. Catal. 39 (2006) 167–174.
[55] L. Jiao, J.R. Regalbuto, The synthesis of highly dispersed noble and base metals on silica via strong electrostatic adsorption: I. Amorphous silica, J. Catal. 260 (2008) 329–341.
[56] X. Zhu, H.-r. Cho, M. Pasupong, J.R. Regalbuto, Charge-enhanced dry impregnation: a simple way to improve the preparation of supported metal catalysts, ACS Catal. 3 (2013) 625–630.
[57] A. Zawadzki, J.D.A. Bellido, A.F. Lucrédio, E.M. Assaf, Dry reforming of ethanol over supported Ni catalysts prepared by impregnation with methanolic solution, Fuel Process. Technol. 128 (2014) 432–440.
[58] P. Munnik, P.E. de Jongh, K.P. de Jong, Recent developments in the synthesis of supported catalysts, Chem. Rev. 115 (2015) 6687–6718.
[59] A.J. van Dillen, R.J.A.M. Terörde, D.J. Lensveld, J.W. Geus, K.P. de Jong, Synthesis of supported catalysts by impregnation and drying using aqueous chelated metal complexes, J. Catal. 216 (2003) 257–264.
[60] B. Harbrecht, S. Thimmaiah, M. Armbrster, C. Pietzonka, S. Lee, Structure and properties of gamma -brass-type Pt_2Zn_{11}, J. Inorg. Gen. Chem. 628 (2002) 2744–2749.
[61] S. Thimmaiah, G.J. Miller, Pd2.28(1)Zn10.37(1)Al0.35(1), a ternary gamma-brass-type structure, Acta Crystallogr. Sect. E Struct. Rep. Online 66 (2010) 1–7.
[62] O. Gourdon, D. Gout, D.J. Williams, T. Proffen, S. Hobbs, G.J. Miller, Atomic distributions in the Γ-brass structure of the Cu-Zn system : a structural and theoretical study, J. Inorg. Chem. 46 (2006) 251–260.
[63] N.K. Mukhopadhyay, D. Mukherjee, S. Bera, I. Manna, R. Manna, Synthesis and characterization of nano-structured Cu–Zn γ-brass alloy, Mater. Sci. Eng.: A 485 (2008) 673–680.
[64] H.Y. Shao, H.R. Xu, Y.T. Wang, X.G. Li, Preparation and hydrogen storage properties of Mg2Ni intermetallic nanoparticles, Nanotechnology 15 (2004) 269–274.
[65] C.S. Spanjers, R.S. Sim, N.P. Sturgis, B. Kabius, R.M. Rioux, In situ spectroscopic characterization of Ni1– x Znx ZnO catalysts and their selectivity for acetylene semihydrogenation in excess ethylene, ACS Catal. 5 (2015) 3304–3315.
[66] A. Onda, T. Komatsu, T. Yashima, Preparation and catalytic properties of single-phase Ni–Sn intermetallic compound particles by CVD of Sn(CH3)4 onto Ni/silica, J. Catal. 201 (2001) 13–21.
[67] V. Milanova, T. Petrov, I. Denev, I. Markova, Nanocomposites based on intermetallic nanoparticles template synthesized using different supports, J. Chem. Technol. Metall. (2013) 48.

[68] S. Sarkar, R. Jana, U.V. Suchitra, B. Waghmare, S. Kuppan, S. Sampath, C. Peter, ordered Pd2Ge intermetallic nanoparticles as highly efficient and robust catalyst for ethanol oxidation, Chem. Mater. 27 (2015) 7459–7467.
[69] M. Martin-Gonzalez, A.L. Prieto, M.S. Knox, R. Gronsky, T. Sands, A.M. Stacy, Electrodeposition of Bi1-xSbx films and 200-nm wire arrays from a nonaqueous solvent, Chem. Mater. 15 (2003) 1676–1681.
[70] C.C. Koch, J.D. Whittenberger, Mechanical milling/alloying of intermetallics, Intermetallics 4 (1996) 339–355.
[71] Y. Vasquez, Z. Luo, R.E. Schaak, Low-temperature solution synthesis of the non-equilibrium ordered intermetallic compounds Au3Fe, Au3Co, and Au3Ni as nanocrystals, J. Am. Chem. Soc. 130 (2008) 11866–11867.
[72] K. Takanashi, S. Mitani, M. Sano, H. Fujimori, H. Nakajima, A. Osawa, Artificial fabrication of an L1(0)-type ordered FeAu alloy by alternate monatomic deposition, Appl. Phys. Lett. 67 (1995) 1016–1018.
[73] K. Sato, B. Bian, Y. Hirotsu, L1(0) type ordered phase formation in Fe-Au nanoparticles, Jpn. J. Appl. Phys. Part. 2 - Lett. 41 (2002) L1–L3.
[74] R.E. Cable, R.E. Schaak, Solution synthesis of nanocrystalline M − Zn (M = Pd, Au, Cu) intermetallic compounds via chemical conversion of metal nanoparticle precursors, Chem. Mater. 19 (2007) 4098–4104.
[75] R.E. Cable, R.E. Schaak, Low-temperature solution synthesis of nanocrystalline binary intermetallic compounds using the polyol process, Chem. Mater. 17 (2005) 6835–6841.
[76] D.O. Downing, Z. Liu, B.W. Eichhorn, Synthesis of PtSn4 and Ir3Sn7 intermetallic nanoparticles from bimetallic zintl cluster precursors, polyhedron, 103, Part. A (2016) 66–70.
[77] A. Yakymovych, H. Ipser, Synthesis and characterization of pure Ni and Ni-Sn intermetallic nanoparticles, Nanoscale Res. Lett. 12 (2017) 142.
[78] V. Milanova, T. Petrov, O. Chauvet, I. Markova, Study of carbon-based nanocomposites with intermetallic (Co-Sn, Ni-Sn) nanoparticles, Rev. Adv. Mater. Sci. (2014) 37.
[79] A. Ota, M. Armbrüster, M. Behrens, D. Rosenthal, M. Friedrich, I. Kasatkin, F. Girgsdies, W. Zhang, R. Wagner, R. Schlögl, Intermetallic compound Pd_2Ga as a selective catalyst for the semi-hydrogenation of acetylene: from model to high performance systems, J. Phys. Chem. C 115 (2011) 1368–1374.
[80] B.M. Leonard, N.S.P. Bhuvanesh, R.E. Schaak, Low-temperature polyol synthesis of AuCuSn2 and AuNiSn2: using solution chemistry to access ternary intermetallic compounds as nanocrystals, J. Am. Chem. Soc. 127 (2005) 7326–7327.
[81] D.J. Childers, N.M. Schweitzer, S.M.K. Shahari, R.M. Rioux, J.T. Miller, R.J. Meyer, Modifying structure-sensitive reactions by addition of Zn to Pd, J. Catal. 318 (2014) 75–84.
[82] S. Jana, J.W. Chang, R.M. Rioux, Synthesis and modeling of hollow intermetallic Ni–Zn nanoparticles formed by the kirkendall effect, Nano Lett. 13 (2013) 3618–3625.
[83] H.M. Barkholtz, J.R. Gallagher, T. Li, Y. Liu, R.E. Winans, J.T. Miller, D.-J. Liu, T. Xu, Lithium assisted “dissolution–alloying” synthesis of nanoalloys from individual bulk metals, Chem. Mater. 28 (2016) 2267–2277.
[84] J.S. Sun, Z. Wen, L.P. Han, Z.W. Chen, X.Y. Lang, Q. Jiang, Nonprecious intermetallic Al7Cu4Ni nanocrystals seamlessly integrated in freestanding bimodal nanoporous copper for efficient hydrogen evolution catalysis, Adv. Funct. Mater. 28 (2018) 1706127.
[85] X.Y. Lang, G.F. Han, B.B. Xiao, L. Gu, Z.Z. Yang, Z. Wen, Y.F. Zhu, M. Zhao, J.C. Li, Q. Jiang, Mesostructured intermetallic compounds of platinum and non-transition metals for enhanced electrocatalysis of oxygen reduction reaction, Adv. Funct. Mater. 25 (2015) 230–237.
[86] D. Wang, H.L. Xin, R. Hovden, H. Wang, Y. Yu, D.A. Muller, F.J. DiSalvo, H.D. Abruña, Structurally ordered intermetallic platinum–cobalt core–shell nanoparticles with enhanced activity and stability as oxygen reduction electrocatalysts, Nat. Mater. 12 (2012) 81.
[87] T. Cheng, X.-Y. Lang, G.-F. Han, R.-Q. Yao, Z. Wen, Q. Jiang, Nanoporous (Pt1-xFex)3Al intermetallic compounds for greatly enhanced oxygen electroreduction catalysis, J. Mater. Chem. A 4 (2016) 18878–18884.
[88] G.-F. Han, L. Gu, X.-Y. Lang, B.-B. Xiao, Z.-Z. Yang, Z. Wen, Q. Jiang, Scalable nanoporous (Pt1–xNix)3Al intermetallic compounds as highly active and stable catalysts for oxygen electroreduction, ACS Appl. Mater. Interfaces 8 (2016) 32910–32917.
[89] J.C. Bauer, X. Chen, Q. Liu, T.-H. Phan, R.E. Schaak, Converting nanocrystalline metals into alloys and intermetallic compounds for applications in catalysis, J. Mater. Chem. 18 (2008) 275–282.
[90] A.K. Sra, T.D. Ewers, R.E. Schaak, Direct solution synthesis of intermetallic AuCu and AuCu3 nanocrystals and nanowire networks, Chem. Mater. 17 (2005) 758–766.
[91] L.R. Alden, D.K. Han, F. Matsumoto, H.D. Abruna, F.J. DiSalvo, Intermetallic PtPb nanoparticles prepared by sodium naphthalide reduction of metal-organic precursors: electrocatalytic oxidation of formic acid, Chem. Mater. 18 (2006) 5591–5596.
[92] N.H. Chou, R.E. Schaak, Shape-controlled conversion of beta-Sn nanocrystals into intermetallic M-Sn (M = Fe, Co, Ni, Pd) nanocrystals, J. Am. Chem. Soc. 129 (2007) 7339–7345.
[93] L.B. McCusker, R.B. Von Dreele, D.E. Cox, D. Louer, P. Scardi, Rietveld refinement guidelines, J. Appl. Crystallogr. 32 (1999) 36–50.
[94] O. Gourdon, Z. Izaola, L. Elcoro, V. Petricek, G.J. Miller, Structure determination of Two modulated γ-brass structures in the zn − pd system through a (3 + 1)-dimensional space description, Inorg. Chem. 48 (2009) 9715–9722.
[95] V.-A. Edstrom, S. Westman, X-ray determination of the structure of cubic gamma Pd,Zn phase, Acta Chem. Scand. 23 (1969) 279–285.
[96] C.S. Spanjers, A. Dasgupta, M. Kirkham, B.A. Burger, G. Kumar, M.J. Janik, R.M. Rioux, Determination of bulk and surface atomic arrangement in Ni–Zn γ-brass phase at different Ni to Zn ratios, Chem. Mater. 29 (2017) 504–512.
[97] F. Ducastelle, B. Legrand, G. Tréglia, Surface segregation in transition metal alloys from electronic structure to phase portraits, Prog. Theor. Phys. Suppl. 101 (1990) 159–180.
[98] A.V. Ruban, H.L. Skriver, J.K. Nørskov, Surface Segregation Energies in Transition-Metal Alloys, (1999).
[99] K. Yaqoob, J.-C. Crivello, J.-M. Joubert, Comparison of the site occupancies determined by combined rietveld refinement and density functional theory calculations: example of the ternary Mo–Ni–Re σ phase, Inorg. Chem. 51 (2012) 3071–3078.
[100] E. Gliozzo, W.A. Kockelmann, G. Artioli, Neutron diffraction of Cu-Zn-Sn ternary alloys: non-invasive assessment of the compositions of historical bronze/brass copper ternary alloys, J. Appl. Crystallogr. 50 (2017) 49–60.
[101] H. Wei, Z. Jiliang, Z. Lingmin, Rietveld refinement of new ternary compound Al14Dy5Si, J. Rare Earth 24 (2006) 78–81.
[102] W. Xie, G.J. Miller, New Co–Pd–Zn γ-brasses with dilute ferrimagnetism and Co2Zn11 revisited: establishing the synergism between theory and experiment, Chem. Mater. 26 (2014) 2624–2634.
[103] P.A. Midgley, A.S. Eggeman, Precession electron diffraction – a topical review, IUBMB Life 2 (2015) 126–136.
[104] H.H. Brongersma, M. Draxler, M. de Ridder, P. Bauer, Surface composition analysis by low-energy ion scattering, Surf. Sci. Rep. 62 (2007) 63–109.
[105] H.R.J. ter Veen, T. Kim, I.E. Wachs, H.H. Brongersma, Applications of High sensitivity-low energy ion scattering (HS-LEIS) in heterogeneous catalysis, Catal. Today 140 (2009) 197–201.
[106] W. Stadlmayr, C. Rameshan, C. Weilach, H. Lorenz, M. Hävecker, R. Blume, T. Rocha, D. Teschner, A. Knop-Gericke, D. Zemlyanov, S. Penner, R. Schlögl, G. Rupprechter, B. Klötzer, N. Memmel, Temperature-induced modifications of PdZn layers on Pd(111), J. Phys. Chem. C 114 (2010) 10850–10856.
[107] C. Rameshan, W. Stadlmayr, C. Weilach, S. Penner, H. Lorenz, M. Hävecker, R. Blume, T. Rocha, D. Teschner, A. Knop-Gericke, R. Schlögl, N. Memmel, D. Zemlyanov, G. Rupprechter, B. Klötzer, Subsurface-controlled CO2 selectivity of PdZn near-surface alloys in H2 generation by methanol steam reforming, Angew. Chem. Int. Ed. 49 (2010) 3224–3227.
[108] Z.-X. Chen, K.M. Neyman, N. Rösch, Theoretical study of segregation of Zn and Pd in Pd–Zn alloys, Surf. Sci. 548 (2004) 291–300.
[109] G. Weirum, M. Kratzer, H.P. Koch, A. Tamtögl, J. Killmann, I. Bako, A. Winkler, S. Surnev, F.P. Netzer, R. Schennach, Growth and desorption kinetics of ultrathin Zn layers on Pd(111), J. Phys. Chem. C 113 (2009) 9788–9796.
[110] H.P. Koch, I. Bako, G. Weirum, M. Kratzer, R. Schennach, A theoretical study of Zn adsorption and desorption on a Pd(111) substrate, Surf. Sci. 604 (2010) 926–931.
[111] C. Rameshan, W. Stadlmayr, S. Penner, H. Lorenz, L. Mayr, M. Hävecker, R. Blume, T. Rocha, D. Teschner, A. Knop-Gericke, R. Schlögl, D. Zemlyanov, N. Memmel, B. Klötzer, In situ XPS study of methanol reforming on PdGa near-surface intermetallic phases, J. Catal. 290 (2012) 126–137.
[112] N. Kopfle, L. Mayr, P. Lackner, M. Schmid, D. Schidmair, T. Gotsch, S. Penner, B. Kloetzer, Zirconium-palladium interactions during dry reforming of methane, ECS Trans. 78 (2017) 2419–2430.
[113] M.H. Kim, J.R. Ebner, R.M. Friedman, M.A. Vannice, Determination of metal dispersion and surface composition in supported Cu–Pt catalysts, J. Catal. 208 (2002) 381–392.
[114] R.M. Rioux, H. Song, J.D. Hoefelmeyer, P. Yang, G.A. Somorjai, High surface area catalyst design: synthesis characterization, and reaction of platinum nano particles in mesoporous SBA-15 silica, J. Phys. Chem. B 109 (2005) 2192–2202.
[115] R.J. Mikovksy, M. Boudart, H.S. Taylor, Hydrogen-deuterium Exchange on copper, silver, Gold and alloy surfaces 1, J. Am. Chem. Soc. 76 (1954) 3814–3819.
[116] S.L. Bernasek, G.A. Somorjai, Molecular beam study of the mechanism of catalyzed hydrogen–deuterium exchange on platinum single crystal surfaces, J. Chem. Phys. 62 (1975) 3149.
[117] A. Borgschulte, A. Zttel, P. Hug, G. Barkhordarian, N. Eigen, M. Dornheim, R. Bormann, A.J. Ramirez-Cuesta, Hydrogen-deuterium exchange experiments to probe the decomposition reaction of sodium alanate, Phys. Chem. Chem. Phys. : PCCP 10 (2008) 4045–4055.
[118] E. Choren, L. El-Chaar, J.O. Hernández, G. Arteaga, A. Arteaga, J. Sánchez, Catalyst characterization by a probe reaction. Cyclopropane hydrogenolysis and benzene hydrogenation on platinum-alumina catalysts, J. Mol. Catal. 72 (1992) 85–95.
[119] G.-M. Schwab, Metal electrons and catalysis, Trans. Faraday Soc. 42 (1946) 689–697.
[120] G.-M. Schwab, S. Pesmatjoglou, Metal electrons and alloy catalysis. The system gold–cadmium, J. Phys. Colloid Chem. 52 (1948) 1046–1053.
[121] X. Ji, K.T. Lee, R. Holden, L. Zhang, J. Zhang, G.A. Botton, M. Couillard, L.F. Nazar, Nanocrystalline intermetallics on mesoporous carbon for direct formic acid fuel cell anodes, Nat. Chem. 2 (2010) 286.
[122] L.J. Zhang, Z.Y. Wang, D.G. Xia, Bimetallic PtPb for formic acid electro-oxidation, J. Alloys Compd. 426 (2006) 268–271.
[123] L.R. Alden, D.K. Han, F. Matsumoto, H.D. Abruña, F.J. DiSalvo, Intermetallic PtPb nanoparticles prepared by sodium naphthalide reduction of metal-organic precursors: electrocatalytic oxidation of formic acid, Chem. Mater. 18 (2006) 5591–5596.
[124] Global demand of polyethylene to reach 99.6 millions tons in 2018, Pipeline Gas J. 241 (2014).
[125] J. Margitfalvi, L. Guczi, Reactions of acetylene during hydrogenation on Pd black catalyst, J. Catal. 72 (1981) 185–198.
[126] E. Vignola, S.N. Steinmann, A. Al Farra, B. Vandegehuchte, D. Curulla, P. Sautet,

Evaluating the risk of C-C bond formation during selective hydrogenation of acetylene on palladium, ACS Catal. (2018).
[127] F. Studt, F. Abild-Pedersen, T. Bligaard, R.Z. Srensen, C.H. Christensen, J.K. Norskov, Identification of non-precious metal alloy catalysts for selective hydrogenation of acetylene, Science (New York, N.Y.) 320 (2008) 1320–1322.
[128] A. Molnar, A. Sarkany, M. Varga, Hydrogenation of carbon-carbon multiple bonds: chemo-, regio- and stereo-selectivity, J. Mol. Catal. A Chem. 173 (2001) 185–221.
[129] J. Osswald, K. Kovnir, M. Armbrüster, R. Giedigkeit, R.E. Jentoft, U. Wild, Y. Grin, R. Schlögl, Palladium–gallium intermetallic compounds for the selective hydrogenation of acetylene: part II: surface characterization and catalytic performance, J. Catal. 258 (2008) 219–227.
[130] Y. Liu, X. Liu, Q. Feng, D. He, L. Zhang, C. Lian, R. Shen, G. Zhao, Y. Ji, D. Wang, G. Zhou, Y. Li, Intermetallic NixMy (M = Ga and Sn) nanocrystals: a Non-precious metal catalyst for semi-hydrogenation of alkynes, Adv. Mater. 28 (2016) 4747–4754.
[131] S. Furukawa, T. Komatsu, Selective hydrogenation of functionalized alkynes to (E)-alkenes, using ordered alloys as catalysts, ACS Catal. 6 (2016) 2121–2125.
[132] N. Iwasa, N. Takezawa, New supported Pd and Pt alloy catalysts for steam reforming and dehydrogenation of methanol, Top. Catal. 22 (2003) 215–224.
[133] Y.-J. Wang, N. Zhao, B. Fang, H. Li, X.T. Bi, H. Wang, Carbon-supported Pt-based alloy electrocatalysts for the oxygen reduction reaction in polymer electrolyte membrane fuel cells: particle size, shape, and composition manipulation and their impact to activity, Chem. Rev. 115 (2015) 3433–3467.
[134] S. Mukerjee, S. Srinivasan, M.P. Soriaga, Role of structural and electronic properties of Pt and Pt alloys on electrocatalysis of oxygen reduction, J. Electrochem. Soc. 142 (1995) 1409–1422.
[135] M. Shao, Q. Chang, J.-P. Dodelet, R. Chenitz, Recent advances in electrocatalysts for oxygen reduction reaction, Chem. Rev. 116 (2016) 3594–3657.
[136] E. Antolini, J.R.C. Salgado, M.J. Giz, E.R. Gonzalez, Effects of geometric and electronic factors on ORR activity of carbon supported Pt–Co electrocatalysts in PEM fuel cells, Int. J. Hydrogen Energy 30 (2005) 1213–1220.
[137] D.Y. Chung, S.W. Jun, G. Yoon, S.G. Kwon, D.Y. Shin, P. Seo, J.M. Yoo, H. Shin, Y.-H. Chung, H. Kim, B.S. Mun, K.-S. Lee, N.-S. Lee, S.J. Yoo, D.-H. Lim, K. Kang, Y.-E. Sung, T. Hyeon, Highly durable and active PtFe nanocatalyst for electrochemical oxygen reduction reaction, J. Am. Chem. Soc. 137 (2015) 15478–15485.
[138] Q. Li, L. Wu, G. Wu, D. Su, H. Lv, S. Zhang, W. Zhu, A. Casimir, H. Zhu, A. Mendoza-Garcia, S. Sun, New approach to fully ordered fct-FePt nanoparticles for Much enhanced electrocatalysis in acid, Nano Lett. 15 (2015) 2468–2473.
[139] L. Chen, C. Bock, P.H.J. Mercier, B.R. MacDougall, Ordered alloy formation for Pt3Fe/C, PtFe/C and Pt5.75Fe5.75Cuy/CO2-reduction electro-catalysts, Electrochim. Acta 77 (2012) 212–224.
[140] Z. Cui, H. Chen, W. Zhou, M. Zhao, F.J. DiSalvo, Structurally ordered Pt3Cr as oxygen reduction electrocatalyst: ordering control and origin of enhanced stability, Chem. Mater. 27 (2015) 7538–7545.
[141] L. Zou, J. Li, T. Yuan, Y. Zhou, X. Li, H. Yang, Structural transformation of carbon-supported Pt3Cr nanoparticles from a disordered to an ordered phase as a durable oxygen reduction electrocatalyst, Nanoscale 6 (2014) 10686–10692.
[142] H. Schulenburg, E. Müller, G. Khelashvili, T. Roser, H. Bönnemann, A. Wokaun, G.G. Scherer, Heat-treated PtCo3 nanoparticles as oxygen reduction catalysts, J. Phys. Chem. C 113 (2009) 4069–4077.
[143] L. Zou, J. Fan, Y. Zhou, C. Wang, J. Li, Z. Zou, H. Yang, Conversion of PtNi alloy from disordered to ordered for enhanced activity and durability in methanol-tolerant oxygen reduction reactions, Nano Res. 8 (2015) 2777–2788.
[144] A. Nilsson, L.G.M. Pettersson, B. Hammer, T. Bligaard, C.H. Christensen, J.K. Nørskov, The electronic structure effect in heterogeneous catalysis, Catal. Lett. 100 (2005) 111–114.
[145] E. Antolini, Alloy vs. Intermetallic compounds: effect of the ordering on the electrocatalytic activity for oxygen reduction and the stability of low temperature fuel cell catalysts, Appl. Catal. B: Environ. 217 (2017) 201–213.
[146] A. Sarkany, Z. Zsoldos, B. Furlong, J.W. Hightower, L. Guczi, Hydrogenation of 1-butene and 1,3-butadiene mixtures over Pd/ZnO catalysts, J. Catal. 141 (1993) 566–582.
[147] T. Takeshita, W.E. Wallace, R.S. Craig, Rare earth intermetallics as synthetic ammonia catalysts, J. Catal. 44 (1976) 236–243.
[148] B.E. Green, C.S. Sass, L.T. Germinario, P.S. Wehner, B.L. Gustafson, Ester hydrogenation over Pd-Zn/SiO2, J. Catal. 140 (1993) 406–417.
[149] M.L. Cubeiro, J.L.G. Fierro, Partial oxidation of methanol over supported palladium catalysts, Appl. Catal. A 168 (1998) 307–322.
[150] N. Iwasa, T. Mayanagi, N. Ogawa, K. Sakata, N. Takezawa, New catalytic functions of Pd–Zn, Pd–Ga, Pd–In, Pt–Zn, Pt–Ga and Pt–In alloys in the conversions of methanol, Catal. Lett. 54 (1998) 119–123.
[151] S. Furukawa, T. Komatsu, Intermetallic compounds: promising inorganic materials for Well-structured and electronically modified reaction environments for efficient catalysis, ACS Catal. 7 (2017) 735–765.
[152] T. Komatsu, S. Furukawa, Intermetallic compound nanoparticles dispersed on the surface of oxide support as active and selective catalysts, Materi. Trans. 56 (2015) 460–467.
[153] B. Bridier, J. Pérez-Ramírez, Cooperative effects in ternary Cu − Ni − Fe catalysts lead to enhanced alkene selectivity in alkyne hydrogenation, J. Am. Chem. Soc. 132 (2010) 4321–4327.
[154] J.C. Rodríguez, A.J. Marchi, A. Borgna, E. Romeo, A. Monzón, Gas Phase Selective Hydrogenation of Acetylene. Importance of the Formation of Ni-Co and Ni-Cu Bimetallic Clusters on the Selectivity and Coke Deposition, (2001), pp. 37–44.
[155] J.H. Xu, Y.Q. Huang, X.F. Yang, L. He, H.R. Zhou, Q.Q. Lin, T. Zhang, H.R. Geng, Enhancement of acetylene hydrogenation activity Over Ni-Zn bimetallic catalyst by doping with Au, J. Nanosci. Nanotechnol. 14 (2014) 6894–6899.
[156] J. Zhang, T. Wang, P. Liu, Z. Liao, S. Liu, X. Zhuang, M. Chen, E. Zschech, X. Feng, Efficient hydrogen production on MoNi4 electrocatalysts with fast water dissociation kinetics, Nat. Commun. 8 (2017) 15437.
[157] J. Snyder, T. Fujita, M.W. Chen, J. Erlebacher, Oxygen reduction in nanoporous metal–ionic liquid composite electrocatalysts, Nat. Mater. 9 (2010) 904.
[158] X.Y. Lang, H. Guo, L.Y. Chen, A. Kudo, J.S. Yu, W. Zhang, A. Inoue, M.W. Chen, Novel nanoporous au − pd alloy with high catalytic activity and excellent electrochemical stability, J. Phys. Chem. C 114 (2010) 2600–2603.
[159] C. Zhu, D. Du, A. Eychmüller, Y. Lin, Engineering ordered and nonordered porous noble metal nanostructures: synthesis, assembly, and their applications in electrochemistry, Chem. Rev. 115 (2015) 8896–8943.